

Topical Ophthalmic Liposomes Dual-Modified with Penetratin and Hyaluronic Acid for the Noninvasive Treatment of Neovascular Age-Related Macular Degeneration

Chen Sun^{1,*}, Shuyue Zhang^{1,*}, Nan Xu^{1,*}, Kun Liu², Fang Wei², Xiaoqian Zhang¹, Jigang Zhang¹, Shen Gao³, Yuan Yu⁴, Xueying Ding¹

¹Clinical Research Center, Shanghai General Hospital, Shanghai Jiao Tong University School of Medicine, Shanghai, 200080, People's Republic of China;

²Department of Ophthalmology, Shanghai General Hospital, Shanghai Jiao Tong University School of Medicine; Shanghai Key Laboratory of Ocular Fundus Diseases, Shanghai General Hospital, Shanghai Engineering Center for Visual Science and Photomedicine, Shanghai, 200040, People's Republic of China; ³Department of Pharmacy, Changhai Hospital, Second Military Medical University, Shanghai, 200433, People's Republic of China;

⁴Department of Pharmacy, Naval Medical University, Shanghai, 200433, People's Republic of China

*These authors contributed equally to this work

Correspondence: Xueying Ding, Clinical Research Center, Shanghai General Hospital, Shanghai Jiao Tong University School of Medicine, Shanghai, 200080, People's Republic of China, Email dingxueying@126.com; Yuan Yu, Department of Pharmacy, Naval Medical University, Shanghai, 200433, People's Republic of China, Email pharmanyuu@163.com

Introduction: Since intrinsic ocular barrier limits the intraocular penetration of therapeutic protein through eye drops, repeated intravitreal injections of anti-vascular endothelial growth factor (anti-VEGF) agents are the standard therapy for neovascular age-related macular degeneration (nAMD), which are highly invasive and may cause particular ocular complications, leading to poor patient compliance.

Methods: Using Penetratin (Pen) as the ocular penetration enhancer and hyaluronic acid (HA) as the retina-targeting ligand, a dual-modified ophthalmic liposome (Penetratin hyaluronic acid-liposome/Conbercept, PenHA-Lip/Conb) eye drop was designed to non-invasively penetrate the ocular barrier and deliver anti-VEGF therapeutic agents to the targeted intraocular tissue.

Results: PenHA-Lip effectively penetrates the ocular barrier and targets the retinal pigment epithelium via corneal and non-corneal pathways. After a single topical administration of conbercept-loaded PenHA-Lip (PenHA-Lip/Conb), the intraocular concentration of conbercept peaked at 18.74 ± 1.09 ng/mL at 4 h, which is 11.55-fold higher than unmodified conbercept. In a laser-induced choroidal neovascularization (CNV) mouse model, PenHA-Lip/Conb eye drops three times daily for seven days inhibited CNV formation and progression without any significant tissue toxicity and achieved an equivalent effect to a single intravitreal conbercept injection.

Conclusion: PenHA-Lip efficiently and safely delivered conbercept to the posterior eye segment and may be a promising noninvasive therapeutic option for nAMD.

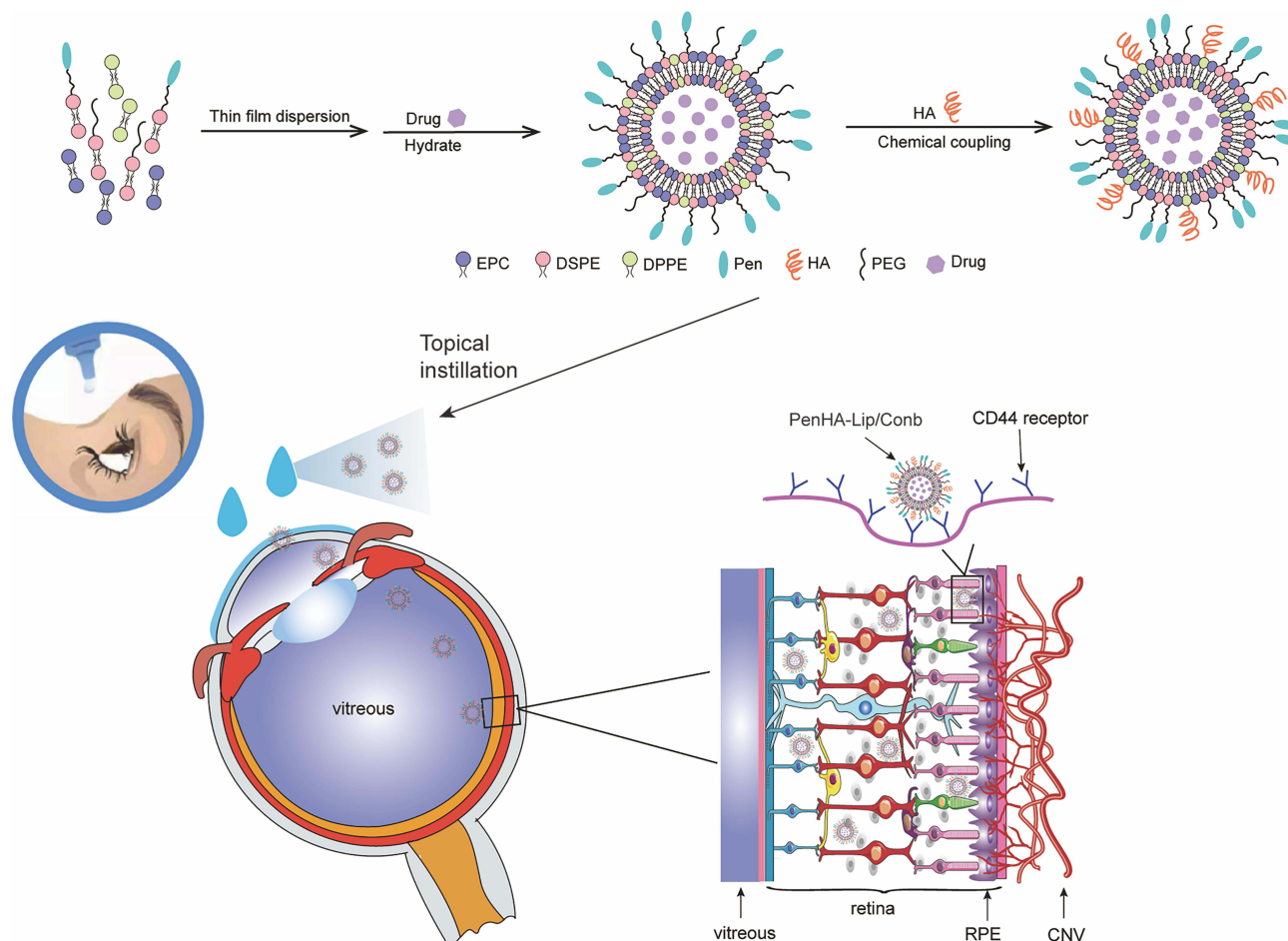
Keywords: ocular drug delivery, dual-modified liposomes, Penetratin, hyaluronic acid, conbercept

Introduction

Globally, age-related macular degeneration (AMD) is a chronic ocular disease that is the leading cause of irreversible vision loss in elderly patients.¹⁻³ In neovascular age-related macular degeneration (nAMD), choroidal neovascularization breaks through Bruch's membrane and grows into the retina through vascular endothelial growth factor (VEGF) stimulation.⁴ The intravitreal injection of anti-vascular endothelial growth factor (anti-VEGF) agents effectively alleviates disease progression by competitively inhibiting the binding of VEGF to its cognate receptors (VEGFR).

Currently, anti-VEGF therapy, mostly administered through intravitreal injection, is the standard treatment for wet AMD.⁵ Conbercept (Conb) is the first self-developed anti-VEGF drug approved in China and is a 143 kDa recombinant

Graphical Abstract



gene fusion protein composed of VEGF-binding domains and the Fc portion of human immunoglobulin G-1. Compared with other anti-VEGF drugs, conbercept has high VEGF-binding specificity and affinity⁶, relatively higher molecular weight (143kD),⁷⁻⁹ and is well tolerated by patients,¹⁰ with its affinity for VEGF is 50-fold and 30-fold higher than that of bevacizumab and ranibizumab, respectively.^{11,12} Therefore, intravitreal therapy is widely used in the Chinese clinical practice. However, this invasive procedure can lead to ocular complications including cataracts, vitreous hemorrhage, retinal detachment, and intraocular inflammation.^{13,14} Repeated injections or even lifelong treatment may further increase psychological and economic burden, resulting in poor patient compliance.² Therefore, less-invasive alternatives should be developed to improve therapeutic compliance of nAMD patients with nAMD.

Topical instillation is a popular method for ocular drug administration; patients can use eye drops by themselves because of their noninvasiveness and convenience.^{15,16} However, dynamic and static ocular barriers, such as tear turnover, nasolacrimal duct drainage, and the cornea and conjunctiva, significantly undermine the drug delivery of eye drops. In particular, the complex barrier properties of the cornea are major challenges in the efficient delivery of drugs to intraocular tissues.¹⁷ For example, hydrophilic and lipophilic properties are required for drugs to penetrate the epithelial and stromal layers of the cornea, respectively.¹⁸ Most anti-VEGF antibodies are characterized by their large molecular size and strong hydrophilicity, which poses limitations on their ability to traverse the blood-retinal barrier.¹⁹ As a result, only a very small percentage (<5%) of drugs enter the eye and function through topical instillation.^{20,21} Enhancing the permeability of drugs through ocular barriers is a primary requirement for improving the bioavailability of drugs after eye drops.

Several preclinical studies have reported that nanocarriers effectively facilitate penetration of small- and large-molecule drugs through corneal barriers.^{22–24} Cell-penetrating peptides (CPPs), a group of peptides from different sources, possess the ability to carry a variety of therapeutic substances, such as liposomes (Lip), proteins, oligonucleotides, and genes across cell membranes.^{25–27} Compared with other penetration enhancers, CPPs, especially the peptide Penetratin, have received considerable attention for ophthalmic drug delivery owing to their low cytotoxicity and excellent biodegradability.²⁸ Penetratin was reported to exhibit the best performance among CPPs in terms of eye permeability and biocompatibility.²⁹ In a study of photodynamic treatment of AMD, the modification of Penetratin on lipoprotein nanoparticle eye drops greatly improved the intraocular permeability of the small-molecule drug verteporfin.³⁰ Liposomes are recognized as the most promising ocular drug delivery carriers, with excellent oil-water partition coefficients similar to those of the cell membrane, which is beneficial for improving ophthalmic drug penetrability.^{31–33} Consequently, Penetratin-modified liposomes may be promising drug carriers for noninvasive ophthalmic treatment.³⁴

Anti-VEGF drugs are used to maintain or improve vision by targeting the neovessels beneath the retina.³⁵ Therefore, drug permeability of the corneal barrier and drug accumulation in the posterior segment of the retina are equally necessary for sufficient nAMD treatment with anti-VEGF agents in a noninvasive manner. However, reaching the ocular fundus at therapeutic concentrations remains a challenge for therapeutic proteins because of their hydrophilic properties and large molecular weights, even when nanotechnology is used to enhance corneal permeation. Hyaluronic acid (HA), a natural glycosaminoglycan that is an important component of the vitreous, may provide the possibility of target and accumulate anti-VEGF drugs in the retina.³⁶ HA specifically interacts with CD44 receptors, which are highly expressed in retinal pigment epithelial cells under disease conditions.^{37,38} Therefore, it is likely that modifying drug carriers with HA could further facilitate the passage of anti-VEGF drugs through the vitreous to target the retina and increase drug concentrations in the posterior segment of the retina.

Given the above understanding, a dual-modified ophthalmic liposome (PenHA-Lip/Conb) eye drop was designed to overcome the ocular barrier and deliver an anti-VEGF drug (conbercept) to the targeted intraocular tissue (Figure 1). Using the thin-film dispersion and chemical coupling method, Penetratin (a penetration enhancer that can pass through the corneal barrier) and HA (a targeting ligand that can improve the mobility of the vector in the vitreous and bind to the CD44 receptor expressed in the retina) were efficiently loaded with hydrophilic conbercept inside the liposome structure. The biocompatibility, corneal penetration, retinal pigment epithelium (RPE) targeting capability, angiogenesis inhibition ability, intraocular distribution, pharmacokinetic behavior, and therapeutic effects of PenHA-Lip/Conb eye drops were evaluated *in vitro* and *in vivo* to develop a novel noninvasive therapeutic option for nAMD.

Materials and Methods

Materials

The following materials were used in this study: Penetratin (CRQIKIWFQNRRMKWKK) with or without carboxy-fluorescein (FAM) labeled (China Peptides, China), conbercept (Chengdu Kanghong Biotechnology, China), cell counting kit-8 (CCK-8 assay) (Shanghai Yisheng Bio-Technology, China), N-(3-Dimethylaminopropyl)-N'-ethylcarbodiimide hydrochloride (EDC) (Shanghai Aladdin Biochemical Technology, China), fluorescein isothiocyanate isomer (FITC)-labeled bovine serum albumin (BSA) (Beijing Solarbio Technology, China), N-hydroxysuccinimide (NHS) (Shanghai Aladdin Biochemical Technology, China), Nile red (Nr) (Shanghai yuanye Biotechnology, China), egg yolk lecithin (EPC) (Shanghai Advanced Vehicle Technology, China), cholesterol (CHOL) (Shanghai Advanced Vehicle Technology, Shanghai, China), dipalmitoyl phosphoethanolamine (DPPE) (Shanghai Advanced Vehicle Technology, China), distearoyl phosphoethanolamine-polyethylene glycol₂₀₀₀ (DSPE-PEG₂₀₀₀) (Shanghai Advanced Vehicle Technology, China), distearoyl phosphoethanolamine-PEG-Penetratin (DSPE-PEG₂₀₀₀-Pen) (China Peptides, China), 1,2-distearoyl-sn-glycero-3-phosphoethanolamine-N-[maleimide(polyethylene glycol)-2000] (DSPE-PEG₂₀₀₀-Mal) (Shanghai Advanced Vehicle Technology, China), HA (120kD, Lifecore Biomedical, USA), recombinant human VEGF₁₆₅ (R&D Systems, USA), human IgG enzyme-linked immunosorbent assay (ELISA) kit (Elabscience Biotechnology, China), paraformaldehyde fix solution (PFA) (Wuhan Servicebio Technology, China), hematoxylin–eosin (HE) staining kit (Beyotime Biotechnology, China), 4',6-diamidino-2-phenylindole (DAPI) (Shanghai Yisheng Bio-Technology, China), growth factor

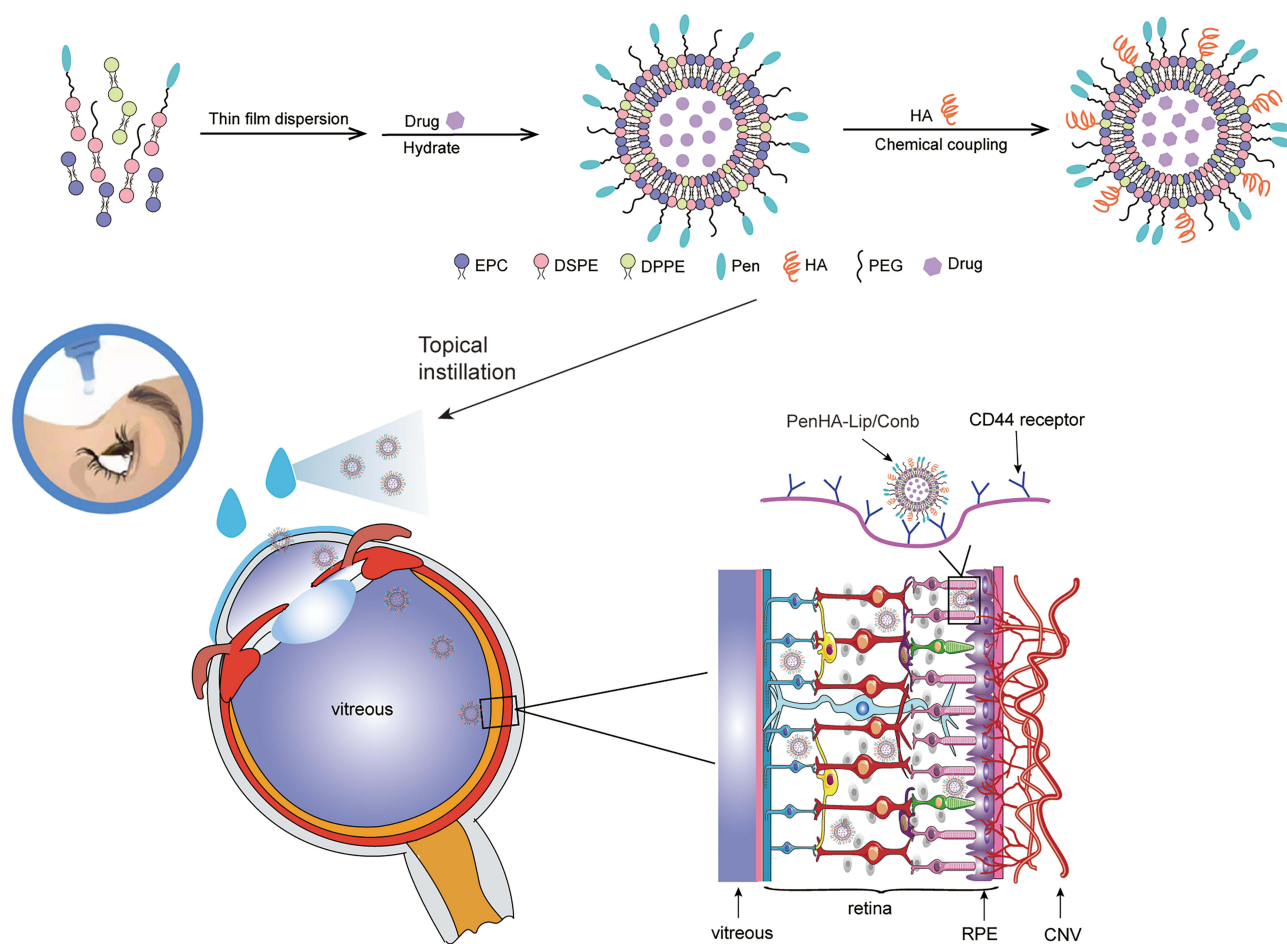


Figure 1 Schematic diagram of the preparation and action mechanism of PenHA-Lip/Comb eye drops.

Abbreviations: HA, hyaluronic acid; EPC, egg yolk lecithin; DSPE, distearoyl phosphoethanolamine; DPPE, dipalmitoyl phosphoethanolamine; PEG, polyethylene glycol; Lip, liposome; Comb, conbercept; Pen, Penetratin; HA, hyaluronic acid; RPE, retinal pigment epithelium; CNV, choroidal neovascularization.

reduced Matrigel and PE mouse anti-human CD44 antibody (BD biosciences, England), and transwell chambers (Corning, USA). All other reagents were of analytical grade.

Cell Lines and Animals

Human corneal epithelial cells (HCEC) were obtained (BeNa Culture Collection Biotech, China). Human retinal pigment epithelial cells (ARPE-19) were kindly provided by Professor Xiaodong Sun (Institute of Ophthalmology of Shanghai General Hospital, China). Human umbilical vein endothelial cells (HUVECs) were purchased from ScienCell Research Laboratories (CA, USA) and cultured in an Endothelial Cell Medium (ECM) (ScienCell, USA). Male C57BL/6J mice (18–20 g) were purchased from the Department of Experimental Animals of the Second Military Medical University (Shanghai, China). Male New Zealand rabbits (1.9–2.5 kg) were provided by the Department of Experimental Animals at the Second Military Medical University (Shanghai, China). All experiments, including animal care, animal experimental procedures and the use of the cell line (eg, ARPE-19), were approved by the Committee of the Shanghai General Hospital. The use and handling of animals also adhered to ethical guidelines outlined in the National Institutes of Health Guide for the Care and Use of Laboratory Animals. All animal experiments and details are shown in [Table S1](#).

Polymer Synthesis and Characterization

Distearoyl phosphoethanolamine-PEG-Penetratin (DSPE-PEG₂₀₀₀-Pen) polymer was synthesized by an addition reaction that conjugated DSPE-PEG₂₀₀₀-Mal to the cysteine residue of Penetratin.³⁹ Briefly, DSPE-PEG₂₀₀₀-Mal and Penetratin

(1:1.5, molar ratio) were dissolved in chloroform at RT. After stirring for 24 h in nitrogen, the solution was filtered and evaporated to remove organic solvent. The residue was re-dissolved in chloroform, re-filtered for purification, evaporated by rotary evaporation, and stored at -20°C . Matrix-assisted laser desorption/ionization time-of-flight mass spectrometry (MALDI-TOF-MS) (Bruker Daltonik GmbH, Bremen, HB, Germany) was used to confirm the final product.³⁹

Liposome Preparation and Characterization

Liposome Preparation

Penetratin-modified liposomes (Pen-Lip) were prepared using the thin-film dispersion method.⁴⁰ Briefly, 10 mg of EPC, 2.5 mg of CHOL, 5 mg of DPPE, 4.5 mg of DSPE-PEG₂₀₀₀, and 17 mg of DSPE-PEG₂₀₀₀-Pen were dissolved in 10 mL dichloromethane: methanol (v: v = 2:1 v/v) and incubated for 10 min. The organic solvent was removed via rotary evaporation under reduced pressure until a thin film was formed. After overnight vacuum drying, the thin films were hydrated in phosphate buffered saline (PBS) (pH 7.4) for 1 h with gentle mixing. The lipid suspension was sonicated for 30 min in an ice bath before extrusion through successive 200 nm and 100 nm microporous filter membranes to obtain an appropriate particle-sized Pen-Lip preparation. The resultant liposomes were subsequently purified through ultracentrifugation at 14, 000 rpm for 30 min at 4°C .

HA-modified liposomes (HA-Lip or PenHA-Lip) were prepared using a carbodiimide coupling reaction.⁴¹ Briefly, 2 mg HA, 2 mg EDC, and 2 mg NHS were dissolved in acetate buffer (pH 4) and incubated at 37°C for 2 h. Then, activated HA was mixed with borate buffer (pH 9) and added to the Lip or Pen-Lip preparation with the weight ratio = 1:1. After stirring at 37°C for 24 h, amide bonds between the carboxyl groups of HA and the amines of DPPE were formed to generate HA modified liposomes.

Plain liposomes (Lip) were formed using the same method but without DSPE-PEG₂₀₀₀-Pen addition. Drug-loaded and fluorescence-labeled liposomes were prepared using a similar method but with minor modifications. FAM-labeled liposomes (Pen-Lip/FAM) were prepared by replacing DSPE-PEG₂₀₀₀-Pen with FAM-labeled DSPE-PEG₂₀₀₀-Pen. Nr-labelled liposomes (Lip/Nr, Pen-Lip/Nr, HA-Lip/Nr, PenHA-Lip/Nr) were formed by adding Nr to the organic solution before solvent evaporation. To prepare the drug-loaded liposomes (PenHA-Lip/Conb, PenHA-Lip/FITC-BSA), PBS solutions containing conbercept or FITC-labeled BSA were used as hydration solutions.

Liposome Characterization

Liposome particle size and zeta potential were determined using a Zetasizer Nano ZS90 (Malvern Instruments Ltd., UK). Liposome morphology was observed using a transmission electron microscope (TEM, JEM-2010, JEOL, Japan) after staining with 2% sodium phosphotungstate solution for 2 min. The entrapment efficiency (EE) and drug loading (DL) of PenHA-Lip/Conb were determined by ultracentrifugation with centrifugation at 14,000 rpm for 30 min. Conbercept concentrations were determined using a human IgG ELISA kit and calculated using the following equations:

$$\text{EE}(\%) = \frac{(\text{weight of total drug} - \text{weight of drug in the supernatant})}{\text{weight of total drug}} \times 100\%$$

$$\text{DL}(\%) = \frac{(\text{weight of total drug} - \text{weight of drug in the supernatant})}{\text{weight of liposomes}} \times 100\%$$

In order to investigate the stability of PenHA-Lip/Conb liposomes under storage conditions (4°C) and physiological conditions (37°C), we used PBS as the culture medium. The particle size of liposomes was measured at different time points. The freshly prepared liposomes were dispersed in PBS. Samples were taken at predetermined time points (0 d, 2 d, 4 d, 6 d, 8 d, 10 d, 12 d, 14 d). The average particle size of the liposomes was determined using a Zetasizer Nano ZS90 (Malvern Instruments Ltd., UK).

The drug-release characteristics of PenHA-Lip/Conb and Lip/Conb were evaluated using dialysis. Liposomes were sealed in dialysis bags, then immersed in 40 mL release medium (PBS buffer containing 0.1% Tween 80, pH 7.4 and 6.3, respectively), and shaken gently at 37°C for 48 h at 150 rpm under light-proof conditions. The release medium (1 mL release) was sampled at predetermined time points (30 min, 1 h, 2 h, 3 h, 4 h, 6 h, 8 h, 12 h, 24 h, and 48 h), and an equal

volume of fresh medium was added. Conbercept concentrations in the extracted samples were determined using a human IgG ELISA kit, and drug release was calculated using the following equation:

$$\text{Drug release(\%)} = \frac{\text{amount of released conbercept}}{\text{total amount of conbercept}} \times 100\%$$

Ex vivo Corneal Penetration

The ability of different liposomes to penetrate isolated rabbit corneas was evaluated using a diffusion cell device (TK-6H1, Kaikai Science and Technology, China) with BSA as the model drug to mimic macromolecular protein drugs. Ex vivo rabbit corneas were horizontally placed between the donor and receptor chambers with the epithelial surface in contact with the donor solution. The donor chamber contained 3 mL free BSA or BSA-loaded liposome solution, whereas the receptor chamber contained an equal volume of PBS. The solutions in the donor chamber and receptor chambers were preheated and maintained at 37°C with gentle stirring. Sample aliquots (100 µL) were collected from the receptor chamber every 30 min for 4 h, followed by successive addition of an equal volume of PBS. The BSA concentrations of the extracted samples were measured using a spectrophotometer (Hitachi, F7000, Japan) and used to calculate the apparent permeability coefficient (P_{app} , $\text{cm} \cdot \text{s}^{-1}$) according to the following equation:

$$P_{app} = \frac{\Delta Q}{(\Delta t_0 \cdot A \cdot 3600)}$$

$\Delta Q/\Delta t$ is the change in BSA concentration with time, c_0 is the initial BSA concentration (4 mg/mL) in the donor chamber, A is the diffusion area of the mounted cornea in contact with the solution (0.785 cm^2 , and 3600 is the conversion factor (s).

In vitro Cellular Uptake

Using confocal microscopy and flow cytometry, in vitro cellular uptake of different liposomes labeled with Nr was evaluated in ARPE-19 cells. For qualitative confocal microscopy, ARPE-19 cells were seeded in 24-well plates at a density of 5×10^4 cells/well. After 24 h incubation at 37°C in a 5% CO_2 humidified atmosphere, the culture medium was replaced with serum-free medium containing Nr-labeled liposomes (Lip/Nr, Pen-Lip/Nr, HA-Lip/Nr, PenHA-Lip/Nr), followed by further incubation for 4 h. After washing in cold PBS containing 1000 IU/mL heparin to remove extracellular bound liposomes, cells were fixed in 4% PFA for 30 min. The nuclei were stained with DAPI for 15 min, and the cells were observed using a confocal laser scanning microscope (Leica, Germany).

For quantitative flow cytometry analysis, ARPE-19 cells were seeded in 12-well plates at a density of 1×10^6 cells/well and processed as previously described. After washing in cold PBS containing 1000 IU/mL heparin to remove extracellular bound liposomes, the cells were collected, resuspended in 500 µL PBS, and analyzed by flow cytometry. For targeted inhibition studies, ARPE-19 cells were pre-incubated with 10 mg/mL HA to competitively inhibit the CD44 receptor. After a 4 h incubation with Nr-labeled Pen-Lip and Nr-labeled PenHA-Lip, the cells were treated as previously described, and the mean fluorescence intensity (MFI) was analyzed by flow cytometry (BD Biosciences, England).

In vitro Angiogenic Inhibition Studies

Construction of the Corneal Barrier Model

Transwell inserts were used to construct in vitro corneal barrier models for anti-angiogenic studies ([Figure S1A](#)). In the corneal barrier model, HCEC were seeded in the upper chambers to simulate the corneal barrier, whereas HUVEC were seeded in the lower chambers with the addition of VEGF to simulate the ocular fundus neovascularization microenvironment. HCEC cells (1×10^5 cells/well) were seeded on the upper chamber of collagen-coated transwell inserts (pore size = 0.4 µm) and maintained at 37°C, with the culture medium replaced every other day. Approximately 5–7 days later, the upper chamber medium was removed, and the cells were cultured in an apical air interface for an additional 3–5 days until the culture was three layers thick. The transepithelial electrical resistance was measured, and barriers with values $>300 \Omega \cdot \text{cm}^2$ were successfully constructed.

Cell Proliferation Assay

The antiproliferative effects of PenHA-Lip/Conb on HUVECs were evaluated using the CCK-8 assay. HUVECs were seeded in 96-well plates at a density of 5×10^4 cells/mL in the ECM. After 24 h of incubation, the culture medium was replaced with fresh ECM or ECM containing conbercept, Lip/Conb, and PenHA-Lip/Conb (conbercept concentrations = 30, 60, 120, 250, 500, and 1000 $\mu\text{g/mL}$), with or without 5 ng/mL VEGF₁₆₅ and incubated for another 24 h. The unadministered group served as the negative control and the VEGF₁₆₅ stimulated group served as the positive control. Then, 10 μL of CCK-8 solution was added to each well, and the absorbance of each well was measured at 450 nm using a microplate reader after 1 h of incubation.

Cell Migration Assay

Transwell migration and wound healing assays were performed to evaluate the anti-migratory effects of PenHA-Lip/Conb in HUVEC.

For the transwell migration assay (Figure S1B), HUVEC were seeded in the upper chamber of transwell inserts (pore size = 8 μm) at a density of 1×10^5 cells/mL. Conbercept, Lip/Conb, Pen-Lip/Conb, and PenHA-Lip/Conb (conbercept concentration = 1 mg/mL) were added to the upper chamber of the transwell inserts, whereas serum-free medium, with or without 25 ng/mL VEGF₁₆₅, was added to the lower chambers. After a 6 h incubation at 37°C, non-migrating cells on the upper surface were wiped away with sterile cotton swabs. Migrated cells on the lower surface were fixed in 4% PFA for 30 min, stained with 0.1% crystal violet for 15 min, imaged using an inverted fluorescence microscope (Leica, Germany), and counted using the ImageJ software.

In the wound healing assay (Figure S1C), HUVEC were seeded in 24-well plates at a density of 3×10^5 cells/mL and cultured to 100% confluence. Cell scratch tests were performed by wounding the cell monolayer with a sterile pipette tip, and transwell inserts containing the constructed corneal barrier models were placed above each well. Then, 200 μL of medium containing conbercept, Lip/Conb, Pen-Lip/Conb, and PenHA-Lip/Conb (conbercept concentration = 1 mg/mL) was added to the upper chambers of the transwell inserts, while 600 μL of medium, with or without 50 ng/mL VEGF₁₆₅, was added to the lower chambers. The scratched area before and after the addition of different liposomes for 6 h was observed using an inverted fluorescence microscope (Leica, Germany), and the cell scratch closure rate was calculated using the ImageJ software.

Tube Formation Assay

A tube formation assay was conducted to investigate the antiangiogenic ability of PenHA-Lip/Conb in HUVEC (Figure S1D). Pre-chilled 24-well plates were coated with 250 μL growth factor-reduced matrigel and incubated at 37°C for 30 min until solidification. HUVEC were seeded on Matrigel at a density of 2×10^5 cells/mL, and transwell inserts containing the constructed corneal barrier models were placed above each well. Then, 200 μL of medium containing conbercept, Lip/Conb, Pen-Lip/Conb, and PenHA-Lip/Conb (conbercept concentration = 1 mg/mL) was added to the upper chamber of the transwell inserts, while 600 μL serum-free medium, with or without 25 ng/mL VEGF₁₆₅, was added to the lower chamber. After a 4 h incubation, tube formation images were captured using an inverted fluorescence microscope (Leica, Germany), and the image intensities were measured using ImageJ software.

Ocular Penetration Path and RPE Targeting Study of PenHA-Lip

The ocular penetration pathway and RPE-targeting ability of PenHA-Lip through eye drops were studied by observing the fluorescence distribution of FAM-labeled liposomes (PenHA-Lip/FAM) in C57BL/6J mice.

For the ocular penetration path study, male mice were randomly divided into two groups ($n = 3$ per group). One group was treated with 5 μL PenHA-Lip/FAM eye drops *in vivo*, and the eyes were isolated after 30 min. In the other group, mice were euthanized, and their eyes were isolated for immediate immersion in PenHA-Lip/FAM solution for 30 min *ex vivo*. Subsequently, the removed eyes in each group were fixed in 4% PFA for 24 h and prepared into frozen slices. The nuclei were stained with DAPI, and the slices were observed using a confocal laser scanning microscope (Leica, Germany).

For the RPE targeting study, male mice were euthanized after the instillation of 5 μ L PenHA-Lip/FAM eye drops for 1 h. Then, the eyes were removed, and frozen slices were prepared. After a 1 h incubation in blocking buffer (10% goat serum in PBS) at room temperature, slices were incubated with rabbit anti-CD44 antibody (Guangdong Original Biotechnology, China) (1:1000 dilution) at 4°C overnight in the dark. After washing with PBS, the slices were incubated with a Cy3-labeled goat anti-rabbit secondary antibody (Guangdong Original Biotechnology, China) (1:500 dilution) for 1 h. The nuclei were counterstained with DAPI, and the slices were observed using a confocal laser scanning microscope (Leica, Germany).

Intraocular Distribution of Macromolecular Cargos in PenHA-Lip

The in vivo intraocular distribution and retention time of macromolecular cargo carried by PenHA-Lip eye drops were evaluated in C57BL/6J mice using FITC-labeled BSA as the model drug. 5 μ L of PBS (control), free BSA, Lip/BSA, and PenHA-Lip/BSA were dropped onto the corneal surface of the mouse eyes once every 10 min, three times. After the last administration, mice were sacrificed at 30 min, 1 h, 3 h, 6 h, 12 h, and 24 h. The eyes were removed, fixed in 4% PFA for 1 h, and transferred to a sucrose solution by gradually increasing the concentration from 10% to 30% for overnight dehydration. Frozen sections were dyed with DAPI and observed under an inverted fluorescence microscope.

Ocular Pharmacokinetic Behavior of PenHA-Lip/Conb Eye drops

Conbercept works by slowly diffusing into the vitreous and binding excess VEGF in the eye. To study the ocular pharmacokinetic behavior of PenHA-Lip/Conb eye drops, C57BL/6J mice were treated with 5 μ L PenHA-Lip/Conb eye drops (conbercept concentration = 10 mg/mL), and their eyes were isolated at predetermined time points (30 min, 1 h, 2 h, 4 h, 8 h, 12 h, and 24 h). The vitreous body of each isolated eye was harvested and ground in 110 μ L sterile PBS. After a 30 min centrifugation step at 14,000 rpm at 4°C, the concentration in supernatant was determined using a human IgG ELISA kit.

To compare the drug delivery efficiency between different eye drops, C57BL/6J mice were randomly divided into three groups for a 5 μ L conbercept, Lip/Conb, and PenHA-Lip/Conb eye drop treatment; then, mice eyes were isolated at 4 h, and the free conbercept concentrations in isolated eyes of each group were determined following the above procedures.

In vivo Therapeutic Evaluation of PenHA-Lip/Conb

Laser-induced choroidal neovascularization (CNV) in mice is preferred as the standard model for experimental studies on AMD over non-human primates and rabbits due to several key advantages,⁴² such as higher success rate, cost-effective, demonstrate faster disease progression, and share retinal structural similarities with humans. In this study, laser-induced CNV models were established using C57BL/6J mice for therapeutic evaluation. Male mice were anesthetized by intraperitoneal injection of 1% pentobarbital sodium with tropicamide (Santen, Japan) to dilate the pupils. Bruch's membrane-choroid rupture was induced by laser photocoagulation using a 532 nm wavelength laser (360 mW at 100 ms) (Coherent, USA), approximately one disc diameter away from the optic disc. The formation of bubbles and clear boundaries indicated Bruch's membrane-choroid rupture and the successful establishment of a laser-induced CNV model.

Laser-induced CNV model mice were randomly divided into five groups to receive the following treatments (Figure 2): (1) eye drop: 5 μ L PBS three times a day (*t.i.d.*) for 7 days, (2) eye drop: 5 μ L conbercept solution *t.i.d.* for 7 days, (3) eye drop: 5 μ L Lip/Conb *t.i.d.* for 7 days, (4) eye drop: 5 μ L PenHA-Lip/Conb *t.i.d.* for 7 days, and (5) intravitreal injection (IVT): 2 μ L conbercept solution for a single administration, conbercept concentration of each formulation was 10 mg/mL. The therapeutic effect in each group was assessed through FFA, immunofluorescence staining of the RPE-choroid-scleral complex, and HE staining of CNV lesions.

First, in vivo fluorescence leakage of CNV lesions was observed using FFA on day 7. After mydriasis and intraperitoneal anesthesia, the mice in each group were intraperitoneally injected with 100 μ L of 10% fluorescein sodium and placed on a confocal laser fundus angiography system (Heidelberg, Germany). The optic discs of the mice were moved to the straight center of the visual field for FFA with the retinal imaging microscopy (Micron IV, Phoenix Research Laboratories), contrast images were captured, and the fluorescence leakage areas were measured using the

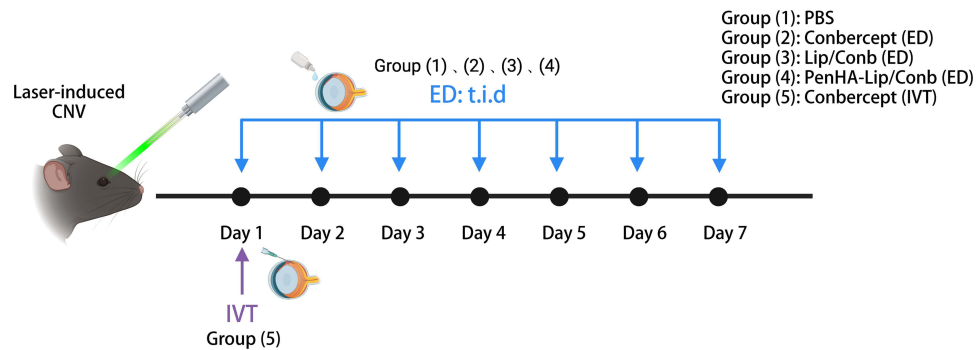


Figure 2 Schematic diagram of the in vivo therapeutic procedure for laser-induced CNV mice ($n = 3$).

Abbreviations: CNV, choroidal neovascularization; IVT, intravitreal injection; ED, eye drop; PBS, phosphate buffered saline; Lip, liposome; Comb, conbercept; Pen, Penetratin; HA, hyaluronic acid; *t.i.d.*, three times a day.

ImageJ software (National Institutes of Health, Bethesda, MD, USA). The fundus was visualized using slit-lamp biomicroscopy (Methocel; Ciba Vision, Wessling, Germany).

Second, CNV lesions were measured by immunofluorescence analysis of the vascular endothelial cell marker isolectin B₄ immunofluorescence analysis. The mouse eyes were removed and placed in 4% PFA for 2 h after heart perfusion by 4% PFA. RPE-choroid-sclera complexes were prepared after removing the anterior segment of the eye and the neural retina. After being radially cutting into 4–6 flaps, RPE-choroid-sclera complexes were immersed in blocking buffer for 1 h at room temperature and then incubated with isolectin B₄ antibody (Vector, USA) (1:1000 dilution) overnight at 4°C, flat-mounted and observed using a fluorescence microscope (Leica, Germany). The CNV lesion areas were measured using ImageJ software.

Third, morphological and pathological changes in the retinal pathological tissues were observed by HE staining on day 7. Mouse eyes were extracted, immediately placed in 4% PFA for over 24 h, serially sliced into sections, stained with HE staining kit, and observed using a fluorescence microscope (Leica, Germany).

Biocompatibility Evaluation

In vitro Cytotoxicity

The cytotoxicity of blank liposomes (Lip, HA-Lip, Pen-Lip, PenHA-Lip) against cells was evaluated using a CCK-8 assay. HCEC and ARPE-19 cells were seeded in 96-well plates at a density of 5×10^3 cells/well. After 24 h incubation (37°C in 5% CO₂), the culture medium was replaced with serum-free medium containing different liposome concentrations (12.5, 25, 50, 125, 250, 500, and 1000 µg/mL) and further incubated for 24 h. Then, 10 µL of CCK-8 solution was added to the wells and incubated for 1 h. The absorbance was measured at 450 nm using a microplate reader (Thermo Fisher Scientific, Waltham, MA, USA).

Ex vivo Rabbit Corneal Toxicity

After ex vivo corneal penetration experiments, the toxicity of liposomes to isolated rabbit corneas was evaluated using corneal hydration values (ΔH) and histopathological staining. Corneas were carefully removed from the diffusion device, and the peripheral scleral tissue was removed and separated into two sections. One section was weighed before and after 48 h drying at 65°C, and ΔH was calculated according to the following equation:

$$\Delta H = \frac{(m_0 - m_1)}{m_0} \times 100\%$$

m_0 and m_1 the corneal weights before and after drying, respectively. The other section was fixed in 4% PFA, HE stained, and observed using a light microscope (Leica, Germany).

In vivo Mouse Ocular Tissue Toxicity

CNV areas were stained with hematoxylin and eosin to evaluate the ocular safety of the liposomes. On day 7 after laser photocoagulation with or without drug administration (untreated, BSA, Lip/BSA, HA-Lip/BSA, Pen-Lip/BSA, PenHA-Lip/BSA), C57BL/6J mice were euthanized. The eyes were immediately removed, placed in 4% PFA for >24 hours, and serially sliced. The largest CNV lesions were stained with HE. To evaluate ocular safety, the cornea, conjunctiva, ciliary body, and retina were embedded in paraffin and stained with HE for histopathological assessment. All the slices were observed under a light microscope (Leica, Germany).

Statistical Analysis

Data are presented as the mean \pm standard deviation (SD). Statistical significance was evaluated using one-way ANOVA. Statistical significance was set at $p < 0.05$.

Results and Discussion

Liposome Characterization

Penetratin was covalently conjugated to DSPE-PEG₂₀₀₀-Mal via an addition reaction between a cysteine residue and maleimide (Figure S2). The molecular weight (MW) of Penetratin (MW = 2837), DSPE-PEG₂₀₀₀-Mal (MW \approx 2900), and DSPE-PEG₂₀₀₀-Pen were determined using electron spray ionization-mass spectrograph (ESI-MS) and MALDI-TOF-MS (Figure S3). MALDI-TOF-MS results demonstrated the successful synthesis of DSPE-PEG₂₀₀₀-Pen, which coincided with a theoretical molecular weight of approximately 5700. The particle size and zeta potential values of the liposomes in this study were determined using dynamic light scattering method and are shown in Table S2. The particle sizes of HA-Lip, Pen-Lip, and PenHA-Lip were larger than that of Lip, suggesting the successful modification of Penetratin and HA. Meanwhile, Lip had a negative zeta potential of -3.1 ± 0.4 mV, while Pen-Lip had a positive zeta potential of 6.6 ± 1.5 mV, this phenomenon provided evidence that the positive-charged Penetratin was modified on the surface of Lip. When negative-charged HA was further modified on Pen-Lip, the zeta potential of PenHA-Lip reversed to -4.3 ± 0.9 mV, suggesting the successful connection of HA. The particle size of PenHA-Lip/Conb was 152.4 ± 1.3 nm, which was approximately 10 nm larger than that of PenHA-Lip, indicating successful drug encapsulation. Importantly, the particle size, negative surface charge, and spherical shape of PenHA-Lip/Conb are suitable for the basic flow and diffusion conditions in the vitreous, which satisfy different ocular applications (Figure 3A, Table S2). The EE of conbercept in PenHA-Lip/Conb was approximately $45.8\% \pm 2.6\%$ ($n = 3$), similar to the reported data of bevacizumab encapsulation in liposomes.⁴³ And the DL of conbercept in PenHA-Lip/Conb was approximately $10.6\% \pm 2.6\%$ ($n = 3$). The particle size of PenHA-Lip/Conb remained stable at 4°C and 37°C for 14 days (Figure S4A), indicates a good formulation stability. The drug release characteristics of Lip/Conb and PenHA-Lip/Conb were evaluated in neutral and acidic environments (Figure 3B, S4B). Lip/Conb and PenHA-Lip/Conb showed similar drug release profiles at pH 7.4 and 6.3, indicating that the modification of liposome surface and change of pH conditions hardly affected the drug release behavior of conbercept delivered by liposomes.

Ex vivo Corneal Penetration

The ex vivo corneal permeability abilities of different formulations in isolated rabbit corneas were evaluated using FITC-labeled bovine serum albumin (BSA) as the model drug. According to the permeability curves, cumulative penetration of BSA increased in a time-dependent manner (Figure 3C). The P_{app} values in the liposome groups, with or without modification, were significantly greater than those in the free BSA group (Figure 3D), indicating that ocular penetration of BSA was improved by liposome delivery. The P_{app} of the PenHA-Lip/BSA group was 7.7-fold, 2.8-fold, and 1.6-fold greater than that of the free BSA, HA-Lip/BSA, and Pen-Lip/BSA groups, respectively. Therefore, the dual modification of Penetratin and HA in liposomes is an effective method for promoting corneal penetration of macromolecular proteins.

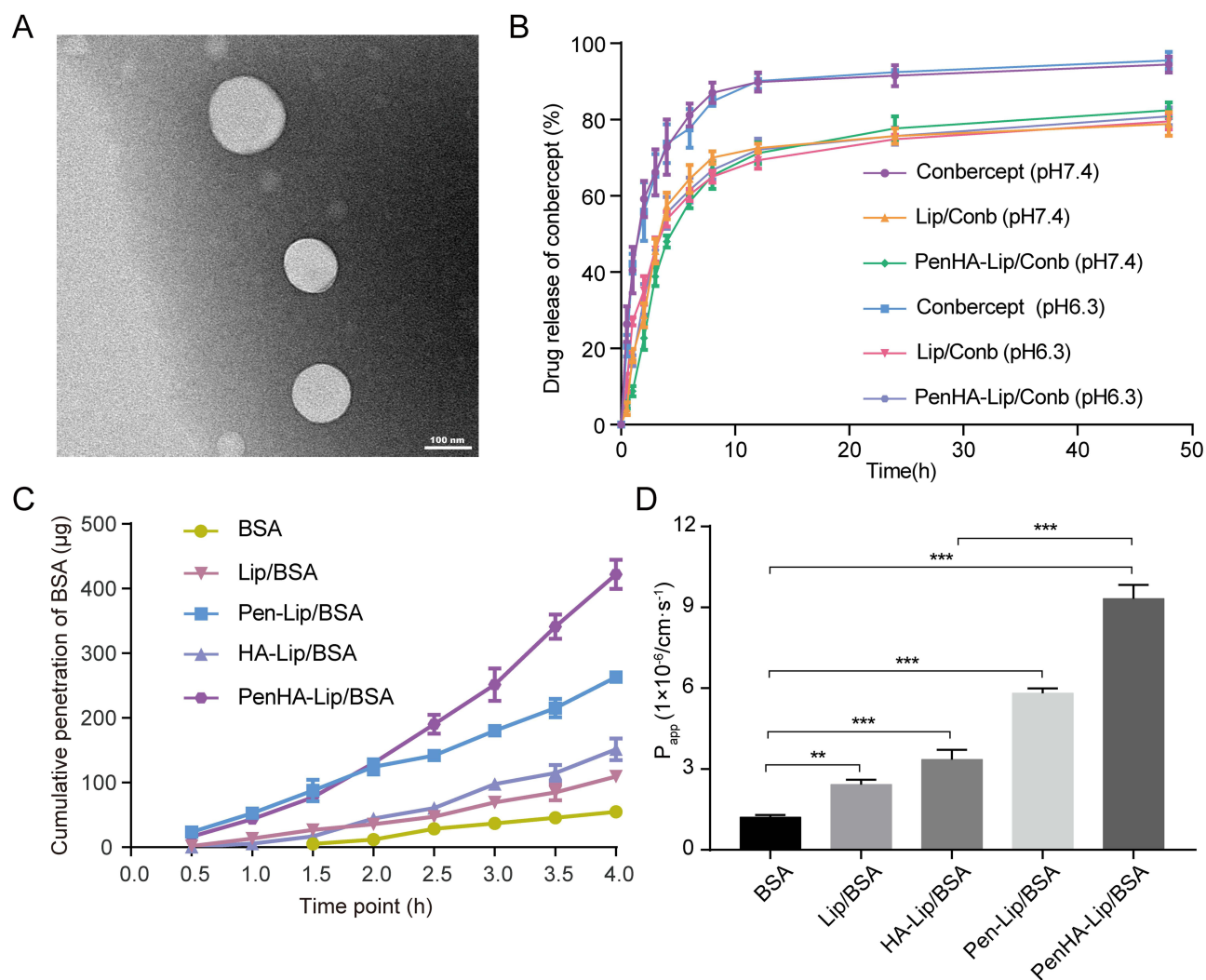


Figure 3 Physical characterization and ex vivo corneal penetration ability. **(A)** TEM image of PenHA-Lip/Conb (scale bar = 100 nm). **(B)** Drug release profiles of conbercept in different formulations at pH 7.4 and 6.3 (n = 3). **(C)** Permeability curves and **(D)** apparent permeability coefficients of macromolecular cargos (BSA) in different liposomes to cross the isolated rabbit corneas (n = 3). Data analyzed by ordinary one-way ANOVA. ** $p < 0.01$, *** $p < 0.001$.

Abbreviations: TEM, transmission electron microscope; PBS, phosphate buffered saline; Lip, liposome; Conb, conbercept; BSA, bovine serum albumin; Pen, Penetratin; HA, hyaluronic acid.

In vitro Cellular Uptake

In vitro cellular uptake properties of different liposomes were evaluated in ARPE-19 cells. As shown in the confocal microscopy images, intracellular fluorescence distribution was observed in ARPE-19 cells after 4 h of incubation with Nr-labeled liposomes (Figure 4A). The PenHA-Lip/Nr group showed the strongest intracellular fluorescence, the HA-Lip/Nr and Pen-Lip/Nr groups showed moderate intracellular fluorescence, and the Lip/Nr group showed weak intracellular fluorescence. Flow cytometry was used to quantitatively detect intracellular uptake in each group (Figure 4B and C). The MFI of the PenHA-Lip/Nr group was 2.10-fold ($P < 0.01$), 1.33-fold ($P < 0.01$), and 1.28-fold ($P < 0.001$) higher than that of Lip-Nr, HA-Lip/Nr, and Pen-Lip/Nr, respectively. Confocal microscopy qualitative analysis and flow cytometry quantitative analysis both demonstrated that ARPE-19 cells had significantly increased cellular uptake of PenHA-Lip when compared with other liposomes.

To verify the cellular targeting ability of different liposomes, ARPE-19 cells were pre-incubated with free HA to competitively inhibit the CD44 receptor. As shown in Figure S5, the MFI in the PenHA-Lip/Nr group was significantly reduced after pre-incubation with HA, but not Pen-Lip/Nr, indicating that the CD44-HA interaction was responsible for the cell-targeting capability of PenHA-Lip. Interestingly, the similar MFI between Pen-Lip/Nr and HA-Lip/Nr suggests

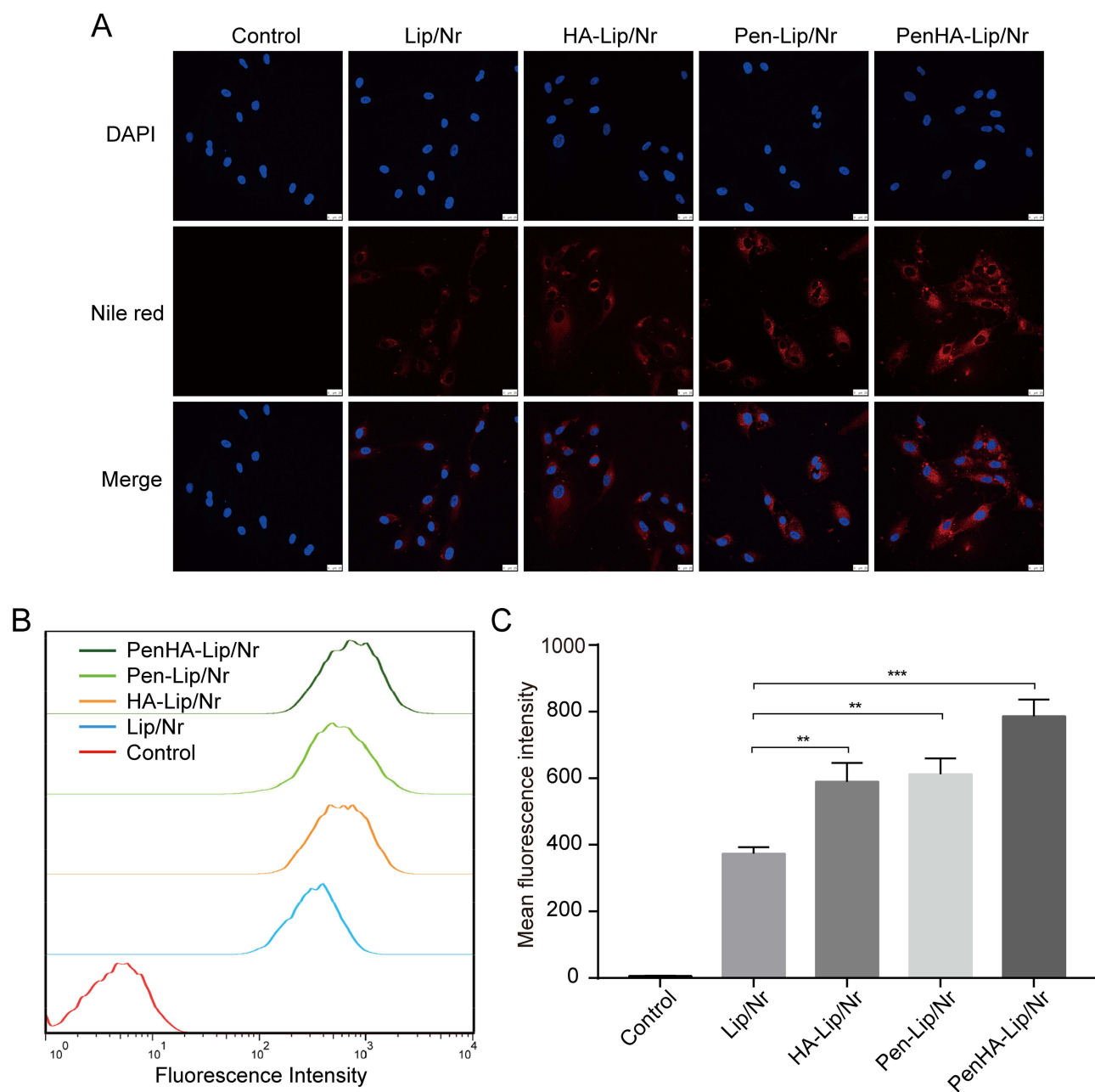


Figure 4 In vitro cellular uptake and targeting ability of different liposomes. **(A)** Laser scanning confocal images of ARPE-19 cells after 4 h incubation with Nr-labeled liposomes (scale bar = 25 μ m). **(B)** Flow cytometry results and **(C)** quantitative analysis of ARPE-19 cells after 4 h incubation with Nr-labeled liposomes (n = 3). Data analyzed by ordinary one-way ANOVA. **p < 0.01, ***p < 0.001.

Abbreviations: ARPE-19, human retinal pigment epithelium cells; Nr, Nile red; DAPI, 4',6-diamidino-2-phenylindole; Lip, liposome; Conb, conbercept; Pen, Penetratin; HA, hyaluronic acid.

that Penetratin also plays a crucial role in enhancing liposome uptake. Therefore, the dual-modified PenHA-Lip possessed the cell penetration capability of Penetratin and cell-targeting ability of HA, which generated the highest cellular uptake in ARPE-19 cells.

In vitro Angiogenic Inhibition

The in vitro anti-angiogenic ability of PenHA-Lip/Conb was evaluated in HUVEC using cell proliferation, cell migration, and tube formation assays.

CCK-8 assay was conducted to evaluate the anti-proliferative effects of PenHA-Lip/Comb on VEGF-induced proliferation induction by VEGF. As shown in Figure 5A, VEGF significantly induced HUVEC proliferation compared to the control group, while conbercept, Lip/Comb, and PenHA-Lip/Comb inhibited cell proliferation induced by VEGF in a dose-dependent manner with similar inhibition curves, suggesting that liposome encapsulation and surface modification of liposomes did not affect the anti-proliferation ability of conbercept in HUVEC.

Transwell migration and wound healing assays were performed to evaluate the anti-migration effects of PenHA-Lip/Comb in HUVEC cells with migration induction by VEGF. The transwell migration assay (Figure S6), conbercept, and drug-loaded liposomes were directly applied to the cells, which exerted a similar inhibitory effect on VEGF-induced migration of HUVECs. In the wound healing assay (Figure 5B–D), conbercept and drug-loaded liposomes crossed the in vitro corneal barrier to exert their action in the lower chamber. Drug-loaded liposomes significantly inhibited HUVEC

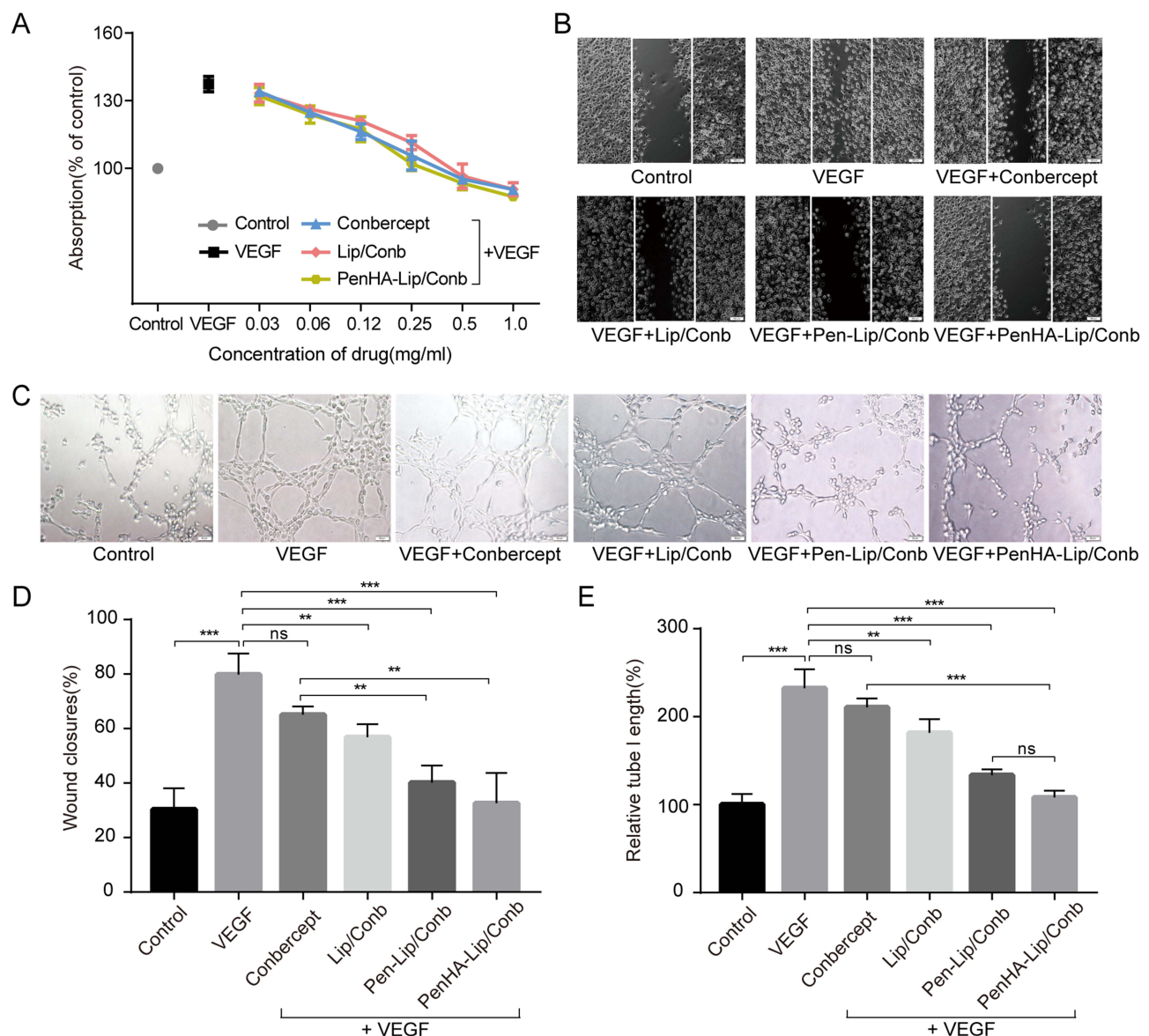


Figure 5 In vitro anti-angiogenic ability of drug-loaded liposomes under the induction of VEGF. **(A)** Proliferation curves of HUVEC cells treated by different conbercept formulations ($n = 3$). **(B)** Representative images of wound healing in HUVEC cells treated by different conbercept formulations (scale bar = 100 μm). **(C)** Representative images of tube formation in HUVEC cells treated by different conbercept formulations for 4 h (scale bar = 50 μm). **(D)** Quantitative analysis of wound closure in different groups after cell scratch ($n = 3$). **(E)** Quantitative analysis of relative tube length in different groups when compared with the control group ($n = 3$). Data analyzed by ordinary one-way ANOVA. ** $p < 0.01$, *** $p < 0.001$.

Abbreviations: VEGF, vascular endothelial growth factor; Lip, liposome; Comb, conbercept; Pen, Penetratin; HA, hyaluronic acid; ns, no significance.

migration, whereas the migration inhibitory effect of free conbercept was quite slight. Moreover, Pen-Lip/Comb and PenHA-Lip/Comb displayed higher anti-migration abilities than Lip/Comb, suggesting that Penetratin modification effectively promoted corneal cell penetration of liposomes.

Tube formation assays were performed to investigate the effect of PenHA-Lip/Comb on the tube-forming ability of HUVEC following VEGF induction (Figure 5C–E). Under the induction of VEGF, clear tube structures were observed in the control, conbercept, and Lip/Comb groups at 4 h, while VEGF-induced tube formation was significantly inhibited in the Pen-Lip/Comb and PenHA-Lip/Comb groups, indicating that Penetratin-modified liposomes effectively penetrated the *in vitro* corneal barrier and delivered conbercept to perform anti-angiogenic action in the lower compartment.

Ocular Penetration Path and RPE Targeting Ability of PenHA-Lip

The ocular penetration pathway and RPE-targeting ability of PenHA-Lip eye drops were studied using FAM-labeled liposomes (PenHA-Lip/FAM) in C57BL/6J mice.

In *in vivo* ocular penetration study (Figure 6A and B), the corneal epithelium, stroma, and endothelium layers showed a wide and distinct fluorescence distribution after single treatment with PenHA-Lip/FAM eye drops in living mice. Meanwhile, the corneal epithelial cytoplasm exhibited strong fluorescence, suggesting that PenHA-Lip penetrated the corneal epithelial layer and was distributed throughout the cornea via the transcellular route (ie, into and through cells). In corneoscleral limbus sections, drug fluorescence was widespread in the cornea, ciliary body, and sclera (Figure 7B). In the *ex vivo* ocular penetration study (Figure 7A), immersing isolated mouse eyes in PenHA-Lip/FAM solution for 30 min only led to fluorescence distribution in the stroma layer and outermost layer of the corneal epithelium with no obvious

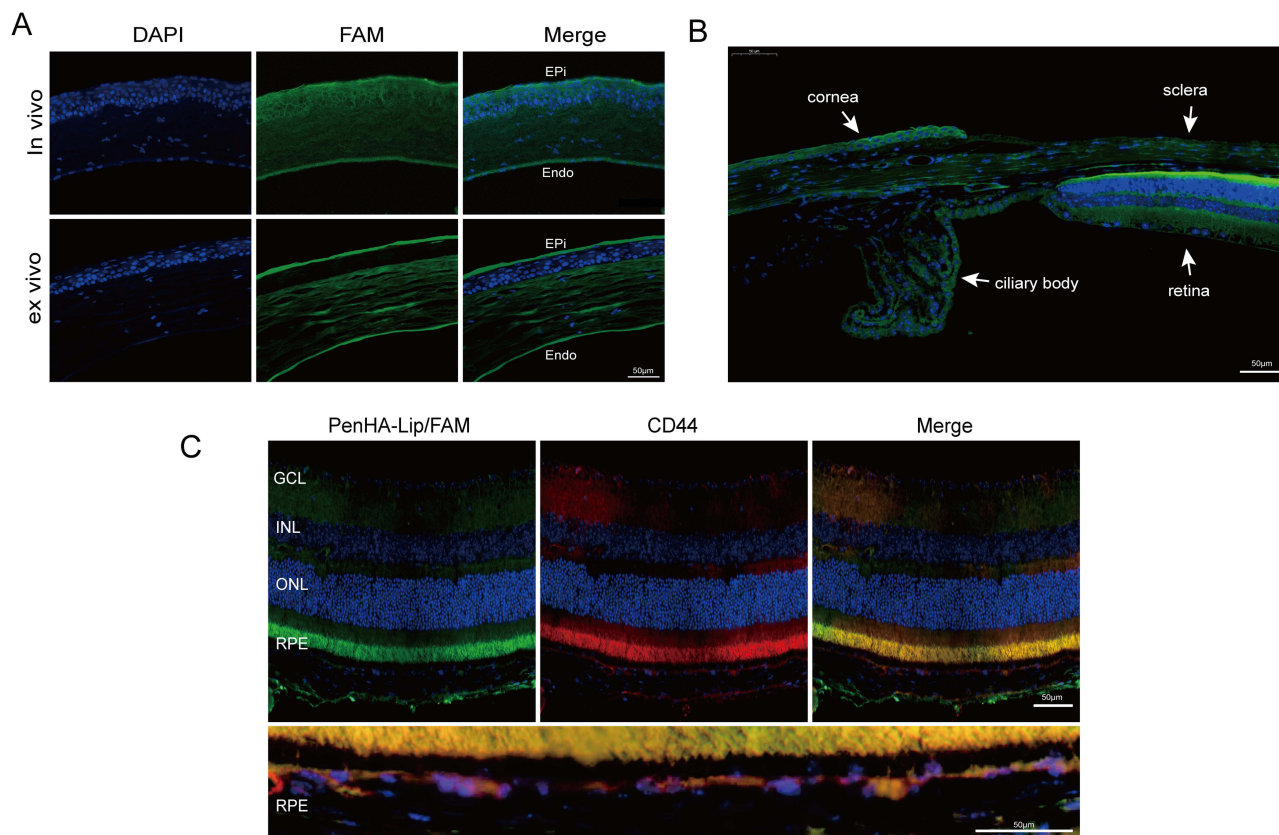


Figure 6 The ocular penetration path and RPE targeting study of PenHA-Lip. **(A)** Confocal images of corneal tissue after PenHA-Lip/FAM topical instillation for *in vivo* and *ex vivo* (scale bar = 50 μm). **(B)** Fluorescence distribution in the corneoscleral limbus after PenHA-Lip/FAM topical instillation *in vivo* (scale bar = 50 μm). **(C)** Fluorescence colocalization of PenHA-Lip/FAM (green fluorescence) and CD44 (red fluorescence) in RPE layer after PenHA-Lip/FAM topical instillation *in vivo* (scale bar = 50 μm).

Abbreviations: Lip, liposome; Comb, conbercept; Pen, Penetratin; HA, hyaluronic acid; FAM, carboxyfluorescein; DAPI, 4',6-diamidino-2-phenylindole; Epi, corneal epithelial layer; Endo, corneal endothelium; GCL, ganglion cell layer; INL, inner nuclear layer; ONL, outer nuclear layer; RPE, retinal pigment epithelium; CD44, homing cell adhesion molecule.

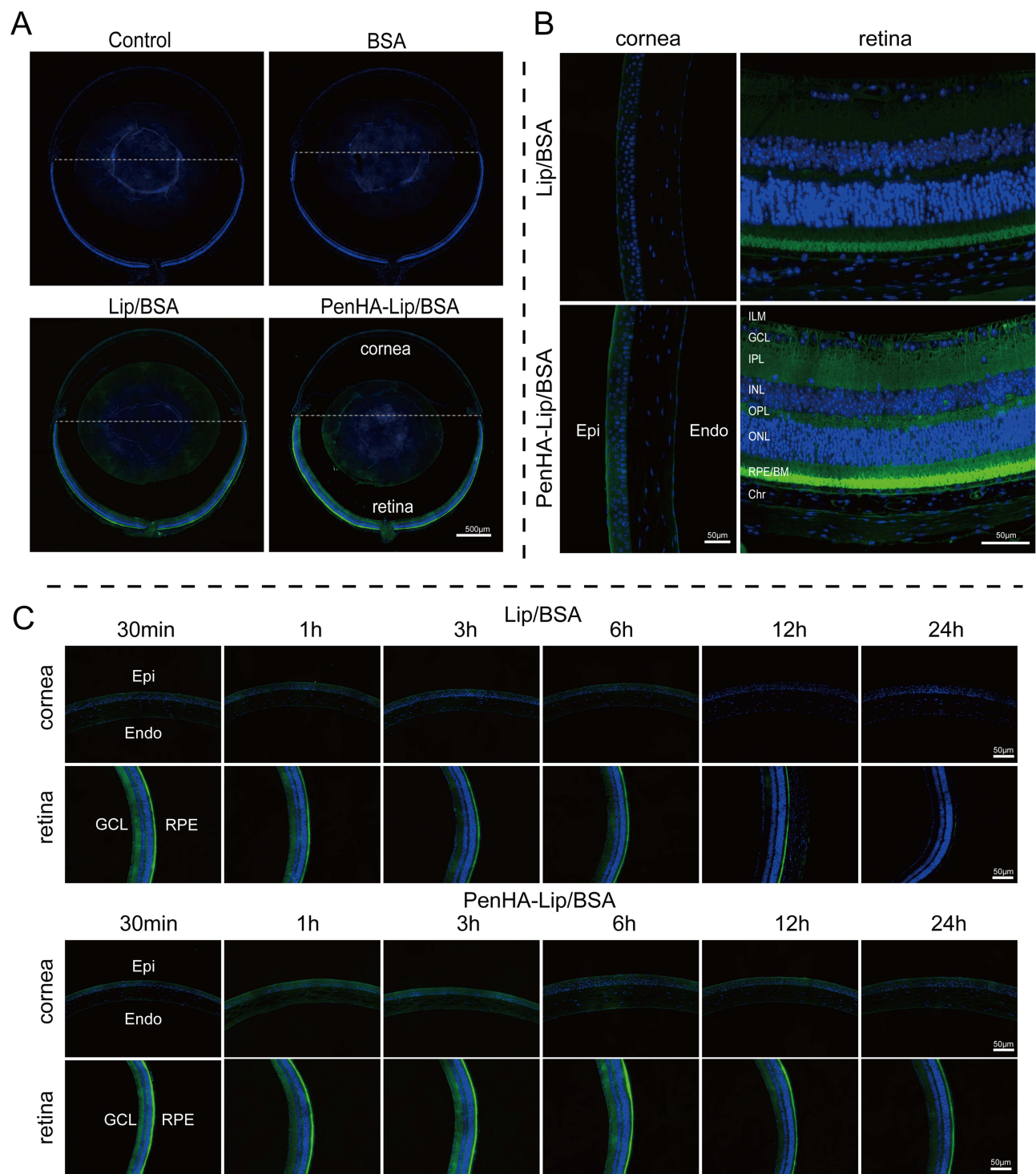


Figure 7 The intraocular distribution of macromolecular cargos carried by different liposome eye drops. **(A)** Fluorescence distribution in the whole eye at 30 min (scale bar = 500 μ m). **(B)** Fluorescence distribution in cornea and retina at 30 min (scale bar = 50 μ m). **(C)** Dynamic fluorescence distribution in cornea and retina during 24 h (scale bar = 50 μ m).

Abbreviations: Lip, liposome; BSA, bovine serum albumin; Pen, Penetratin; HA, hyaluronic acid; Epi, corneal epithelial layer; Endo, corneal endothelium; ILM, internal limiting membrane; GCL, ganglion cell layer; IPL, inner plexiform layer; INL, inner nuclear layer; OPL, outer plexiform layer; ONL, outer nuclear layer; RPE/BM, retinal pigment epithelium/Bruch's membrane complex; Chr, choroid.

fluorescence in the epithelial cytoplasm, suggesting that ex vivo corneal epithelial cells had lost their cellular uptake ability, and PenHA-Lip may also passively diffuse into the cornea via the non-corneal route. In summary, PenHA-Lip eye drops may penetrate the ocular barrier and enter the eye via both the corneal and non-corneal pathways after topical instillation.

For in vivo RPE targeting study, the RPE-targeting ability of PenHA-Lip was further evaluated in vivo. As shown in Figure 6C, yellow fluorescence represents the colocalization of PenHA-Lip/FAM (green fluorescence) and CD44 (red fluorescence) in the RPE layer, suggesting that HA modification could help liposomes target CD44-expressing tissues/cells via the interaction between CD44 and HA. In the enlarged image of the retina, PenHA-Lip/FAM was distinctly present in the cytoplasm of RPE cells, which aligns with the observations that PenHA-Lip effectively targeted CD44-expressing retinal cells in vitro (Figure 4B and C), indicating the high efficiency of PenHA-Lip in overcoming the ocular barriers and targeting the RPE site in vivo.

Intraocular Distribution of Macromolecular Cargos in PenHA-Lip

The in vivo intraocular distribution and retention time of macromolecular cargo carried by PenHA-Lip eye drops were evaluated in C57BL/6J mice using FITC-labeled BSA as the model drug. After topical instillation thrice, distinct fluorescence (green) was observed in the PenHA-Lip/BSA-treated eyes, particularly in the posterior segment, whereas only weak fluorescence was observed in the cornea and retina in the Lip/BSA group, and no fluorescence was observed in the cornea or retina in the free BSA group (Figure 7A). A comparison of the fluorescence distribution between the cornea and retina showed that most of the drugs successfully reached the retina through the delivery of liposomes, particularly accumulated in the RPE layer (Figure 7B). Moreover, the fluorescence of PenHA-Lip/BSA-treated eyes lasted from 30 min to more than 24 h after topical instillation; the fluorescence intensity remained high for the first 6 h and gradually decreased over time. Compared with the Lip/BSA-treated group, PenHA-Lip/BSA showed a longer fluorescence retention time, which may be relevant to its RPE targeting ability (Figure 7C). The targeted accumulation and prolonged retention in the posterior segment of the retina, especially in the RPE layer, indicate the potential of PenHA-Lip as an effective delivery carrier of macromolecular drugs for the precise treatment of ocular fundus diseases.

Ocular Pharmacokinetic Behavior of PenHA-Lip/Conb Eye drops

The pharmacokinetic behavior of conbercept in the vitreous body was measured after single administration of PenHA-Lip/Conb eye drops. As shown in Figure 8A, the conbercept concentration showed a tendency to increase at first and then decrease during 24 h, whose peak value was 18.74 ± 1.09 ng/mL at 4 h. Conbercept concentrations decreased to 12.64 ± 4.61 ng/mL at 8 h and 2.59 ± 0.56 ng/mL at 24 h, suggesting conbercept clearance time of PenHA-Lip/Conb eye drops was longer than 24 h in mice. In addition, the concentration of conbercept in mouse eyes treated with PenHA-Lip/Conb eye drops was significantly higher than that in eyes treated with free drug and Lip/Conb eye drops (Figure 8B), suggesting that PenHA-Lip had the greatest efficiency in drug delivery, which was beneficial for the anti-neovascularization effect of conbercept.

Currently, the common injection dose of conbercept is 0.5 mg/50 μ L in patients with nAMD, which is much higher than the actual effective dose, and the therapeutic effect of a single injection can last 1–3 months.⁴⁴ A preclinical study reported that the conbercept concentration in the vitreous body was 20.28 ± 28.85 ng/mL at 2 days after a single intravitreal injection of 20 μ g conbercept.⁴⁵ In our study, conbercept levels reached 18.74 ± 1.09 ng/mL at 4 h after a single topical instillation of 50 μ g PenHA-Lip/Conb eye drops, which was almost equivalent to the level after a single intravitreal injection ($p > 0.05$). Additionally, conbercept concentrations of PenHA-Lip/Conb eye drops lasted for more than 24 h and peaked at 4 h. Therefore, PenHA-Lip/Conb eye drops were administered three times a day in this study in order to maintain effective therapeutic levels for nAMD treatment.

In vivo Therapeutic Evaluations

After identifying the dosage regimen and achievable drug concentrations, a laser-induced CNV mouse model was established to evaluate the anti-neovascularization effects of PenHA-Lip/Conb eye drops in vivo. FFA assays, isolectin B₄ immunofluorescence staining, and histopathological staining were performed to determine the therapeutic efficacy of

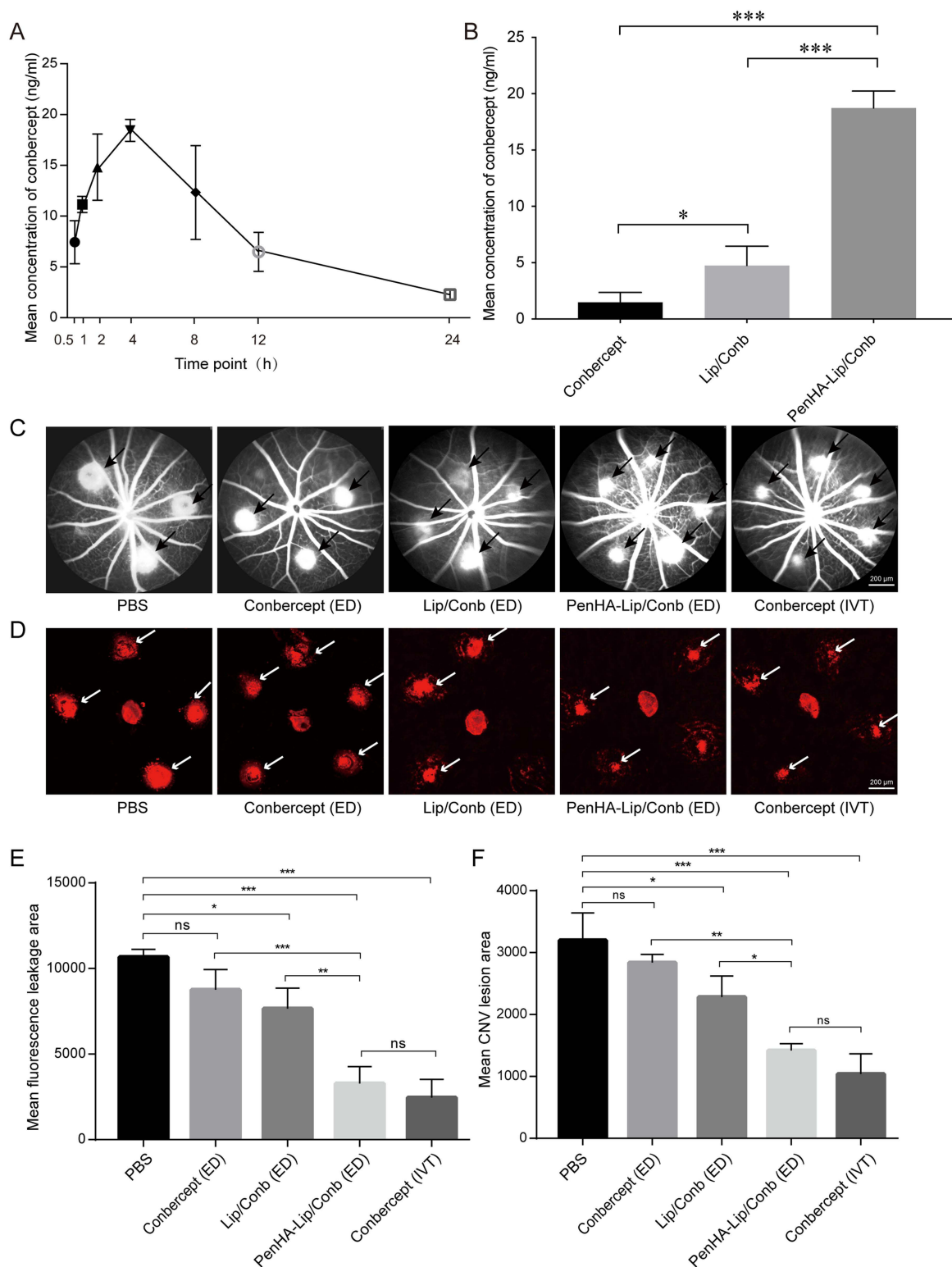


Figure 8 Ocular pharmacokinetic behavior and therapeutic effects of PenHA-Lip/Comb eye drops. **(A)** Ocular pharmacokinetic behavior of PenHA-Lip/Comb eye drops after a single topical instillation ($n = 4$). **(B)** The quantitative comparison of conbercept concentrations at 4 h in different groups ($n = 4$). **(C)** FFA images on day 7 in laser-induced CNV mice treated with eye drops *t.i.d.* or a single intravitreal injection (scale bar = 200 μm). **(D)** Quantitative statistics of fluorescence leakage areas in each group ($n = 3$). **(E)** Representative immunofluorescence images on day 7 in laser-induced CNV mice treated with eye drops *t.i.d.* or a single intravitreal injection (scale bar = 200 μm). **(F)** Quantitative statistics of CNV lesion areas in each group ($n = 3$). The black arrow represents the fluorescence leakage area; the white arrow represents the CNV lesion area. Data analyzed by ordinary one-way ANOVA. * $p < 0.05$, ** $p < 0.01$, *** $p < 0.001$.

Abbreviations: Lip, liposome; Comb, conbercept; Pen, Penetratin; HA, hyaluronic acid; FFA, representative fundus fluorescein angiography; CNV, choroidal neovascularization; *t.i.d.*, three times a day; ED, eye drop; IVT, intravitreal injection; PBS, phosphate-buffered saline.

PenHA-Lip/Conb eye *t.i.d.* for seven days in laser-induced CNV lesions. It is worth noting that genetic susceptibility plays a primary role in the development of human nAMD, whereas the experimental CNV model in this study was an acute injury caused by a certain laser wavelength and relied heavily on inflammation.²⁶ Moreover, mice do not have a defined macula,⁴⁶ so the laser-induced CNV models cannot completely mimic the complexity of the pathology of human nAMD. Nevertheless, a laser-induced CNV model can still be commonly used for the therapeutic evaluation of drugs owing to its anti-neovascularization effects, since neovascularization is a crucial feature of nAMD pathophysiology.

As demonstrated in the FFA assay (Figure 8C and D), following a seven-day period of therapeutic intervention, the fluorescent leakage areas in the PBS, conbercept (ED), Lip/Conb (ED), PenHA-Lip/Conb (ED), and conbercept (IVT) groups were as follows: $10,666 \pm 451$, 8757 ± 1189 , 7661 ± 1193 , 3280 ± 994 , and 2453 ± 1064 , respectively. No significant inhibitory effects of conbercept eye drops on CNV lesion size were observed when compared with the PBS group, whereas CNV lesion size was significantly reduced in the group receiving daily topical instillations of PenHA-Lip/Conb eye drops or a single intravitreal injection of conbercept. Interestingly, no significant differences were observed in the reduction of CNV lesion sizes between the PenHA-Lip/Conb eye drop and conbercept intravitreal groups, suggesting that the bioefficacy of PenHA-Lip/Conb eye drops *t.i.d.* was equivalent to that of a single intravitreal conbercept injection. A similar characteristic was observed in the isolectin B₄ expression analysis (Figure 8E and F). Neovascularization areas were measured and compared using isolectin B₄ as the vascular endothelial cell marker. Quantitative evaluations showed that the CNV areas were significantly reduced by PenHA-Lip/Conb eye drops, whose anti-neovascularization effect was as efficacious as that of a single intravitreal conbercept injection. Based on the encouraging results of continuous 7-day treatment, the PenHA-Lip/Conb eye drops demonstrate significant effectiveness and therapeutic potential, laying a preliminary foundation for subsequent research. Our future plans involve further confirmation of these findings through an extended follow-up period.

Morphological and pathological changes in CNV areas were also observed by HE staining of the retinal tissues. As shown in Figure S7, normal retinas presented an intact structure with clear layers, whereas retinas near CNV lesions became severely detached with deranged inner and outer nuclear layers in the PBS group. In the conbercept eye drop group, RPE and Bruch's membranes were broken, and cells had proliferated from the choroid to the retina, showing typical CNV lesion symptoms. After intervention with daily PenHA-Lip/Conb eye drops and a single intravitreal conbercept injection, the retinas were almost restored to normal structures where the cells were neatly arranged.

Therefore, *in vivo* therapeutic data demonstrated that the CNV areas of the mice that received PenHA-Lip/Conb eye drops *t.i.d.* for 7 days were similar to those of the mice that received a single conbercept intravitreal injection, indicating the therapeutic advantage of PenHA-Lip/Conb eye drops in non-invasively and precisely producing an anti-neovascularization effect in nAMD treatment.

Biocompatibility Evaluation

Liposome biocompatibility was investigated using the CCK-8 assay, ΔH , and histological examinations. Cell viability of HCEC cells and ARPE-19 cells was over 90% at liposome concentrations of 12.5–1000 $\mu\text{g/mL}$, demonstrating good liposome biocompatibility with these cells (Figure 9A and B). The ΔH value of the cornea is a crucial parameter for toxicological assessments following corneal penetration tests. As reported, the ΔH value of a normal healthy cornea is 76–80%, and a ΔH value of 83–92% indicates some degree of damage to the corneal epithelium or endothelium.⁴⁷ As shown in Figure 9C and D, the ΔH values of corneas treated with liposomes were between 78.02% and 80.41%, and a well-defined layered morphology was demonstrated by HE staining, suggesting that liposomes were not toxic to corneas. In addition, laser-induced CNV mice were in good condition with no clinical abnormalities during topical administration of liposomes for *t.i.d.* 7 days, such as eyeball congestion, edema, increased secretion, and turbid refractive medium. No significant difference was observed in the HE staining images of the cornea, conjunctiva, ciliary body, and retina between the liposome and PBS groups (Figure 9E). Thus, PenHA-Lip/Conb eye drops *t.i.d.* showed good ocular biocompatibility for the treatment of ophthalmic diseases.

Since clinical adverse reactions of conbercept are predominantly associated with the injection procedure,^{5,10,48} we focus on designing a drug carrier that primarily addresses safety concerns related to conbercept injection. Despite the short action duration of eye drops compared to direct vitreous injection,⁴⁹ pharmacological and animal studies have also

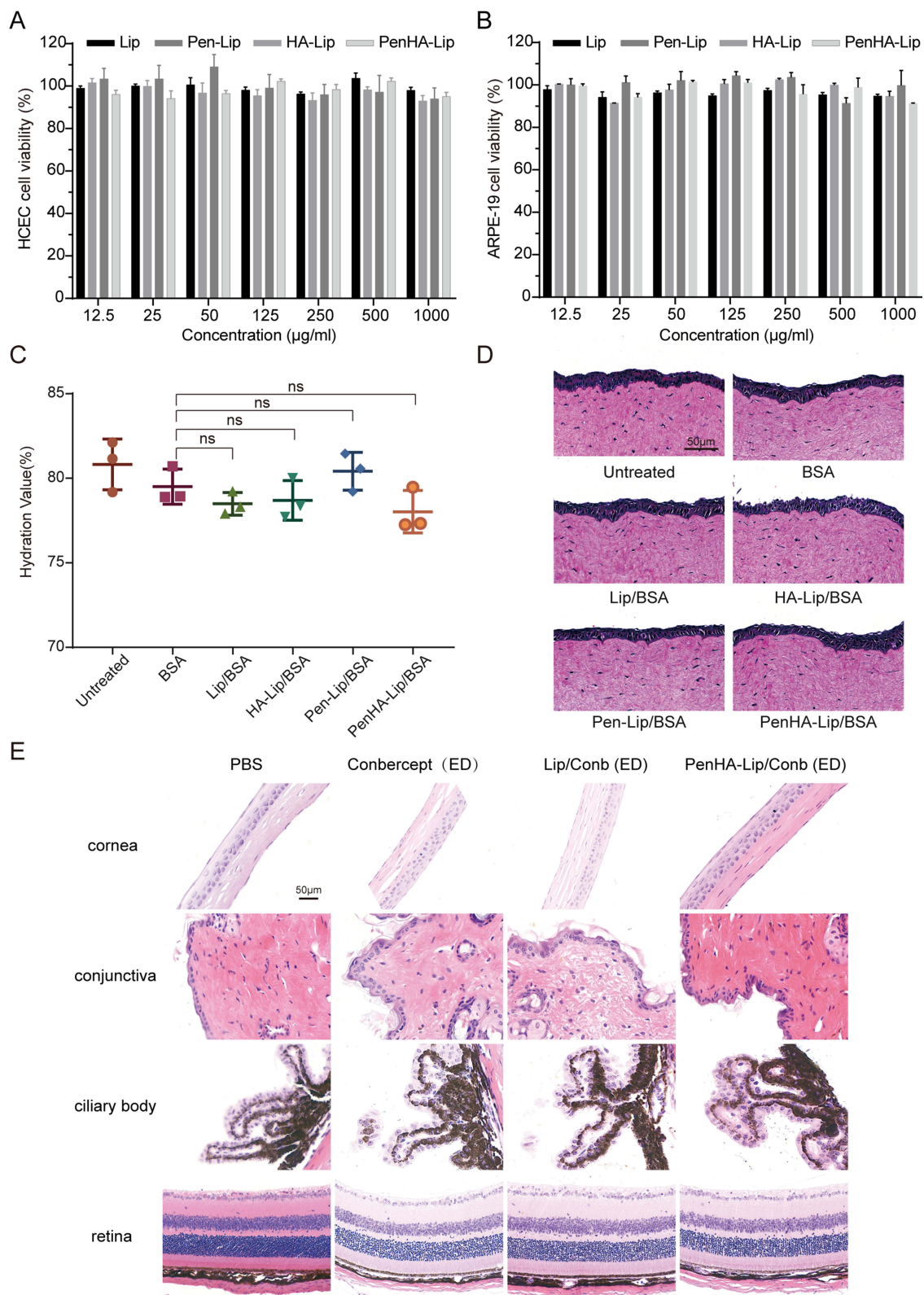


Figure 9 Biocompatibility evaluation of liposomes. Cell proliferation effects of different liposome concentrations on (A) HCEC cells and (B) ARPE-19 cells ($n = 3$). (C) Hydration value ($n = 3$) and (D) HE stained sections of isolated rabbit corneas after the corneal penetration test (scale bar = 50 µm). (E) Histological images of eye tissues on day 7 treated with eye drops *t.i.d.* (scale bar = 50 µm). Data analyzed by ordinary one-way ANOVA.

Abbreviations: Lip, liposome; Comb, conbercept; Pen, Penetratin; HA, hyaluronic acid; HCEC, human corneal epithelial cells; ARPE-19, human retinal pigment epithelium cells; BSA, bovine serum albumin; PBS, phosphate-buffered saline; HE, hematoxylin–eosin staining; *t.i.d.*, three times a day; ED, eye drop; ns, no significance.

validated the feasibility of ocular instillation and its improvement in safety. However, AMD is considered a multifactorial disease, involving a complex interaction between aging, genetic susceptibility, and environmental risk factors.⁵⁰ Hence, monotherapy face limitations, as not all patients respond favorably to anti-vascular endothelial growth factor (VEGF) treatments.⁵¹ An increasing body of research highlights the advantages of conbercept in combination therapies.⁵ Consequently, the application of novel Conbercept eye drops and the identification of effective early biomarkers,⁵² with combined intervention, may potentially emerge as future research directions.

Conclusion

In this study, an ophthalmic liposome dual-modified with Penetratin and HA (PenHA-Lip/Comb) was prepared for noninvasive treatment of nAMD. Specifically, PenHA-Lip eye drops showed high permeability through the ocular barrier with the conjugation of Penetratin and targeted the RPE site with HA modification during topical instillation. In addition, PenHA-Lip/Comb inhibited VEGF-induced HUVEC proliferation, migration, and tube formation, resulting in good antiangiogenic ability. Importantly, PenHA-Lip/Comb eye drops effectively delivered an anti-VEGF agent (conbercept) to the posterior segment of the mouse eyes, and the therapeutic outcome was comparable to that of a single intravitreal injection, with no significant toxicity observed. In summary, our findings in dual-modification liposomes not only reveal a new method for the noninvasive treatment of nAMD but also provide a promising application for other chronic fundus diseases.

Abbreviations

ARPE-19, human retinal pigment epithelium cells; BRVO, branch vein occlusion; BSA, bovine serum albumin; CCK-8, cell counting kit-8; CD44, homing cell adhesion molecule; CHOL, cholesterol; Chr, choroid; CNV, choroidal neovascularization; Comb, conbercept; CPP, cell-penetrating peptides; DAPI, 4,6-diamino-2-phenyl indole; DL, drug loading; DLS, dynamic light scattering; DPPE, dipalmitoyl phosphoethanolamine; DSPE, distearoyl phosphoethanolamine; DSPE-PEG₂₀₀₀, distearoyl phosphoethanolamine-polyethylene glycol₂₀₀₀; DSPE-PEG₂₀₀₀-Mal, 1,2-distearoyl-sn-glycero-3-phosphoethanolamine-N-[maleimide(polyethylene glycol)-2000]; DSPE-PEG₂₀₀₀-Pen, distearoyl phosphoethanolamine-PEG-Penetratin; ECM, endothelial cell medium; ED, eye drop; EDC, N-(3-Dimethylaminopropyl)-N'-ethylcarbodiimide hydrochloride; EE, entrapment efficiency; ELISA, enzyme-linked immunosorbent assay; Endo, corneal endothelium; EPC, egg yolk lecithin; Epi, corneal epithelial layer; ESI-MS, electrospray ionization mass spectrometry; FAM, carboxyfluorescein; FFA, fundus fluorescein angiography; GCL, ganglion cell layer; HA, hyaluronic acid; HA-Lip or PenHA-Lip, HA-modified liposomes; HCEC, human corneal epithelial cells; HE, hematoxylin-eosin staining; HUVEC, human umbilical vein endothelial cells; ILM, internal limiting membrane; INL = inner nuclear layer; IPL, inner plexiform layer; IVT, intravitreal injection; Lip, liposome; MALDI-TOF-MS, matrix-assisted laser desorption/ionization time-of-flight mass spectrometry; MFI, mean fluorescence intensity; MW, molecular weight; nAMD, neovascular age-related macular degeneration; NHS, N-hydroxysuccinimide; Nr, Nile red; Papp, apparent permeability coefficient; ns, no significance; ONL, outer nuclear layer; OPL, outer plexiform layer; PBS, phosphate-buffered saline; PDT, photodynamic therapy; PEG, polyethylene glycol; Pen, Penetratin; Pen-Lip, Penetratin-modified liposomes; Pen-Lip/FAM, FAM-labeled liposomes; PFA, paraformaldehyde fix solution; PLT, photoreceptor layer thickness; PRN, pro re nata; q.w, quaque week; RPE, retinal pigment epithelium; RPE/BM, retinal pigment epithelium/Bruch's membrane complex; *t.i.d.*, three times a day; TEM, transmission electron microscope; VEGF, vascular endothelial growth factor; ΔH , hydration values.

Data Sharing Statement

All data and material are included in the article and its additional files.

Funding

This work was supported by the Interdisciplinary Program of Shanghai Jiao Tong University (No. 0507N17014, China).

Disclosure

The authors declare that they have no competing interests in this work.

References

1. Mitchell P, Liew G, Gopinath B., et al. Age-related macular degeneration. *Lancet*. 2018;392(10153):1147–1159. doi:10.1016/S0140-6736(18)31550-2
2. Chakravarthy U, Peto T. Current perspective on age-related macular degeneration. *JAMA*. 2020;324(8):794–795. doi:10.1001/jama.2020.5576
3. Steinmetz JD, Bourne RRA, Briant PS. Causes of blindness and vision impairment in 2020 and trends over 30 years, and prevalence of avoidable blindness in relation to VISION 2020: the right to sight: an analysis for the global burden of disease study. *Lancet Glob Health*. 2021;9(2):e144–e60. doi:10.1016/S2214-109X(20)30489-7
4. Nguyen QD, Das A, Do DV, et al. Brolucizumab: evolution through preclinical and clinical studies and the implications for the management of neovascular age-related macular degeneration. *Ophthalmology*. 2020;127(7):963–976. doi:10.1016/j.ophtha.2019.12.031
5. Sarkar A, Jayesh Sodha S, Junnuthula V, et al. Novel and investigational therapies for wet and dry age-related macular degeneration. *Drug Discovery Today*. 2022;27(8):2322–2332. doi:10.1016/j.drudis.2022.04.013
6. Nguyen TT, Conbercept GR. (KH-902) for the treatment of neovascular age-related macular degeneration. *Expert Rev Clin Pharmacol*. 2015;8(5):541–548. doi:10.1586/17512433.2015.1075879
7. Holz FG, Dugel PU, Weissgerber G, et al. Single-chain antibody fragment VEGF Inhibitor RTH258 for neovascular age-related macular degeneration: a randomized controlled study. *Ophthalmology*. 2016;123(5):1080–1089. doi:10.1016/j.ophtha.2015.12.030
8. Chen JJ, Ebmeier SE, Sutherland WM, et al. Potential penetration of topical ranibizumab (Lucentis) in the rabbit eye. *Eye*. 2011;25(11):1504–1511. doi:10.1038/eye.2011.225
9. Moreno M, Pow PY, Tabitha TST, et al. Modulating release of ranibizumab and aflibercept from thiolated chitosan-based hydrogels for potential treatment of ocular neovascularization. *Expert Opin Drug Deliv*. 2017;14(8):913–925. doi:10.1080/17425247.2017.1343297
10. Sun Z, Zhou H, Lin B, et al. EFFICACY AND SAFETY OF INTRAVITREAL CONBERCEPT INJECTIONS IN MACULAR EDEMA SECONDARY TO RETINAL VEIN OCCLUSION. *Retina*. 2017;37(9):1723–1730. doi:10.1097/IAE.0000000000001404
11. Zhang M, Zhang J, Yan M, et al. Recombinant anti-vascular endothelial growth factor fusion protein efficiently suppresses choroidal neovascularization in monkeys. *Mol Vis*. 2008;14:37–49.
12. Zhang M, Yu D, Yang C, et al. The pharmacology study of a new recombinant human VEGF receptor-fc fusion protein on experimental choroidal neovascularization. *Pharm Res*. 2009;26(1):204–210. doi:10.1007/s11095-008-9718-9
13. Falavarjani KG, Nguyen QD. Adverse events and complications associated with intravitreal injection of anti-VEGF agents: a review of literature. *Eye (Lond)*. 2013;27(7):787–794. doi:10.1038/eye.2013.107
14. Nuzzi R, Tridico F. Local and systemic complications after intravitreal administration of anti-vascular endothelial growth factor agents in the treatment of different ocular diseases: a five-year retrospective study. *Semin Ophthalmol*. 2015;30(2):129–135. doi:10.3109/08820538.2013.835833
15. Li J, Cheng T, Tian Q, et al. A more efficient ocular delivery system of triamcinolone acetonide as eye drop to the posterior segment of the eye. *Drug Deliv*. 2019;26(1):188–198. doi:10.1080/10717544.2019.1571122
16. Souto EB, Dias-Ferreira J, López-Machado A, et al. Advanced formulation approaches for ocular drug delivery: state-of-the-art and recent patents. *Pharmaceutics*. 2019;11(9):9. doi:10.3390/pharmaceutics11090460
17. Wong CW, Wong TT. Posterior segment drug delivery for the treatment of exudative age-related macular degeneration and diabetic macular oedema. *Br J Ophthalmol*. 2019;103(10):1356–1360. doi:10.1136/bjophthalmol-2018-313462
18. Janagam DR, Wu L, Lowe TL. Nanoparticles for drug delivery to the anterior segment of the eye. *Adv Drug Deliv Rev*. 2017;122:31–64. doi:10.1016/j.addr.2017.04.001
19. Jiang D, Xu T, Zhong L, et al. Research progress of VEGFR small molecule inhibitors in ocular neovascular diseases. *Eur. J. Med. Chem*. 2023;257:115535. doi:10.1016/j.ejmech.2023.115535
20. Gorantla S, Rapalli VK, Waghule T, et al. Nanocarriers for ocular drug delivery: current status and translational opportunity. *RSC Adv*. 2020;10(46):27835–27855. doi:10.1039/D0RA04971A
21. Jünemann A, Chorągiewicz T, Ozimek M, et al. Drug bioavailability from topically applied ocular drops. Does drop size matter? *Ophthalmol J*. 2016;1(1):29–35. doi:10.5603/OJ.2016.0005
22. Luo LJ, Nguyen DD, Lai JY. Dually functional hollow ceria nanoparticle platform for intraocular drug delivery: a push beyond the limits of static and dynamic ocular barriers toward glaucoma therapy. *Biomaterials*. 2020;243:119961. doi:10.1016/j.biomaterials.2020.119961
23. Jiang K, Hu Y, Gao X, et al. Octopus-like flexible vector for noninvasive intraocular delivery of short interfering nucleic acids. *Nano Lett*. 2019;19(9):6410–6417. doi:10.1021/acs.nanolett.9b02596
24. Zhao X, Seah I, Xue K, et al. Antiangiogenic nanomicelles for the topical delivery of aflibercept to treat retinal neovascular disease. *Adv Mater*. 2022;34(25):e2108360. doi:10.1002/adma.202108360
25. Dos Santos Rodrigues B, Kanekiyo T, Singh J. ApoE-2 brain-targeted gene therapy through transferrin and penetratin tagged liposomal nanoparticles. *Pharm Res*. 2019;36(11):161. doi:10.1007/s11095-019-2691-7
26. De Cogan F, Hill LJ, Lynch A, et al. Topical delivery of anti-VEGF drugs to the ocular posterior segment using cell-penetrating peptides. *Invest Ophthalmol Vis Sci*. 2017;58(5):2578–2590. doi:10.1167/iovs.16-20072
27. Nakase I, Akita H, Kogure K, et al. Efficient intracellular delivery of nucleic acid pharmaceuticals using cell-penetrating peptides. *Acc Chem Res*. 2012;45(7):1132–1139. doi:10.1021/ar200256e
28. Moiseev RV, Morrison PWJ, Steele F, et al. Penetration enhancers in ocular drug delivery. *Pharmaceutics*. 2019;11(7):7. doi:10.3390/pharmaceutics11070321
29. Liu C, Tai L, Zhang W, et al. Penetratin, a potentially powerful absorption enhancer for noninvasive intraocular drug delivery. *Mol Pharm*. 2014;11(4):1218–1227. doi:10.1021/mp400681n
30. Ran M, Deng Y, Yan J, et al. Neovascularization-directed bionic eye drops for noninvasive renovation of age-related macular degeneration. *Chem Eng J*. 2022;450:138291. doi:10.1016/j.cej.2022.138291

31. Lai S, Wei Y, Wu Q, et al. Liposomes for effective drug delivery to the ocular posterior chamber. *J Nanobiotechnology*. 2019;17(1):64. doi:10.1186/s12951-019-0498-7
32. Khalil M, Hashmi U, Riaz R, et al. Chitosan coated liposomes (CCL) containing triamcinolone acetonide for sustained delivery: a potential topical treatment for posterior segment diseases. *Int J Biol Macromol*. 2020;143:483–491. doi:10.1016/j.ijbiomac.2019.10.256
33. Navarro-Partida J, Altamirano-Vallejo JC, Lopez-Naranjo EJ, et al. Topical triamcinolone acetonide-loaded liposomes as primary therapy for macular edema secondary to branch retinal vein occlusion: a pilot study. *J Ocul Pharmacol Ther*. 2020;36(6):393–403. doi:10.1089/jop.2019.0143
34. Xu J, Khan AR, Fu M, et al. Cell-penetrating peptide: a means of breaking through the physiological barriers of different tissues and organs. *J Control Release*. 2019;309:106–124. doi:10.1016/j.jconrel.2019.07.020
35. Parravano M, Costanzo E, Scondotto G, et al. Anti-VEGF and other novel therapies for neovascular age-related macular degeneration: an update. *BioDrugs*. 2021;35(6):673–692. doi:10.1007/s40259-021-00499-2
36. Bishop PN. Structural macromolecules and supramolecular organisation of the vitreous gel. *Prog Retin Eye Res*. 2000;19(3):323–344. doi:10.1016/S1350-9462(99)00016-6
37. Murata M, Horiuchi S. Hyaluronan synthases, hyaluronan and its CD44 receptors in the posterior segment of rabbit eye. *Ophthalmologica*. 2005;219(5):287–291. doi:10.1159/000086113
38. Liu NP, Roberts WL, Hale LP, et al. Expression of CD44 and variant isoforms in cultured human retinal pigment epithelial cells. *Invest Ophthalmol Vis Sci*. 1997;38(10):2027–2037.
39. Zhang Q, Tang J, Fu L, et al. A pH-responsive α -helical cell penetrating peptide-mediated liposomal delivery system. *Biomaterials*. 2013;34(32):7980–7993. doi:10.1016/j.biomaterials.2013.07.014
40. Ji T, Lang J, Wang J, et al. Designing liposomes to suppress extracellular matrix expression to enhance drug penetration and pancreatic tumor therapy. *ACS Nano*. 2017;11(9):8668–8678. doi:10.1021/acsnano.7b01026
41. Tang M, Svirskis D, Leung E, et al. Can intracellular drug delivery using hyaluronic acid functionalised pH-sensitive liposomes overcome gemcitabine resistance in pancreatic cancer? *J Control Release*. 2019;3:305.
42. Grossniklaus HE, Kang SJ, Berglin L. Animal models of choroidal and retinal neovascularization. *Prog Retinal Eye Res*. 2010;29(6):500–519. doi:10.1016/j.preteyeres.2010.05.003
43. Abrishami M, Zarei-Ghanavati S, Soroush D, et al. Preparation, characterization, and in vivo evaluation of nanoliposomes-encapsulated bevacizumab (avastin) for intravitreal administration. *Retina*. 2009;29(5):699–703. doi:10.1097/IAE.0b013e3181a2f42a
44. Liu K, Song Y, Xu G, et al. Conbercept for treatment of neovascular age-related macular degeneration: results of the randomized phase 3 phoenix study. *Am J Ophthalmol*. 2019;197:156–167. doi:10.1016/j.ajo.2018.08.026
45. Du L, Peng H, Wu Q, et al. Observation of total VEGF level in hyperglycemic mouse eyes after intravitreal injection of the novel anti-VEGF drug conbercept. *Mol Vis*. 2015;21:185–193.
46. Shah RS, Soetikno BT, Lajko M, et al. A mouse model for laser-induced choroidal neovascularization. *J Vis Exp*. 2015;106:e53502.
47. Dai Y, Zhou R, Liu L, et al. Liposomes containing bile salts as novel ocular delivery systems for tacrolimus (FK506): in vitro characterization and improved corneal permeation. *Int J Nanomed*. 2013;8:1921–1933. doi:10.2147/IJN.S44487
48. Del Amo EM, Rimpelä AK, Heikkinen E, et al. Pharmacokinetic aspects of retinal drug delivery. *Prog Retinal Eye Res*. 2017;57:134–185. doi:10.1016/j.preteyeres.2016.12.001
49. Maurice DM. *Pharmacology of the Eye*. Berlin, Heidelberg: Springer; 1984:19–116.
50. Fleckenstein M, Keenan TDL, Guymer RH, et al. Age-related macular degeneration. *Nat Rev Dis Primers*. 2021;7(1):31. doi:10.1038/s41572-021-00265-2
51. Joo J-H, Kim H, Shin J-H, et al. Aqueous humor cytokine levels through microarray analysis and a sub-analysis based on optical coherence tomography in wet age-related macular degeneration patients. *BMC Ophthalmol*. 2021;21(1):399. doi:10.1186/s12886-021-02152-6
52. Zekavat SM, Sekimitsu S, Ye Y, et al. Photoreceptor layer thinning is an early biomarker for age-related macular degeneration: epidemiologic and genetic evidence from UK Biobank OCT data. *Ophthalmology*. 2022;129(6):694–707. doi:10.1016/j.ophtha.2022.02.001

International Journal of Nanomedicine

Dovepress

Publish your work in this journal

The International Journal of Nanomedicine is an international, peer-reviewed journal focusing on the application of nanotechnology in diagnostics, therapeutics, and drug delivery systems throughout the biomedical field. This journal is indexed on PubMed Central, MedLine, CAS, SciSearch®, Current Contents®/Clinical Medicine, Journal Citation Reports/Science Edition, EMBase, Scopus and the Elsevier Bibliographic databases. The manuscript management system is completely online and includes a very quick and fair peer-review system, which is all easy to use. Visit <http://www.dovepress.com/testimonials.php> to read real quotes from published authors.

Submit your manuscript here: <https://www.dovepress.com/international-journal-of-nanomedicine-journal>